

Potent, Orally Bioavailable and Efficacious Macrocyclic Inhibitors of Factor XIa. Discovery of Pyridine-Based Macrocycles Possessing Phenylazole Carboxamide P1 Groups

James R. Corte, Donald J. P. Pinto, Tianan Fang, Honey Osuna, Wu Yang, Yufeng Wang, Amy Lai, Charles Clark, Jung-Hui Sun, Richard A. Rampulla, Arvind Mathur, Mahammed Kaspady, Premsai Rai Neithnadka, Yi-Xin Li, Karen A Rossi, Joseph E Myers, Steven Sheriff, Zhen Lou, Timothy W. Harper, Christine S. Huang, Joanna J Zheng, Jeffrey M. Bozarth, Yiming Wu, Pancras C Wong, Earl Crain, Dietmar A Seiffert, Joseph M Luetgten, Patrick Lam, Ruth R. Wexler, and William R Ewing
J. Med. Chem., **Just Accepted Manuscript** • DOI: 10.1021/acs.jmedchem.9b01768 • Publication Date (Web): 13 Dec 2019

Downloaded from pubs.acs.org on December 13, 2019

Just Accepted

“Just Accepted” manuscripts have been peer-reviewed and accepted for publication. They are posted online prior to technical editing, formatting for publication and author proofing. The American Chemical Society provides “Just Accepted” as a service to the research community to expedite the dissemination of scientific material as soon as possible after acceptance. “Just Accepted” manuscripts appear in full in PDF format accompanied by an HTML abstract. “Just Accepted” manuscripts have been fully peer reviewed, but should not be considered the official version of record. They are citable by the Digital Object Identifier (DOI®). “Just Accepted” is an optional service offered to authors. Therefore, the “Just Accepted” Web site may not include all articles that will be published in the journal. After a manuscript is technically edited and formatted, it will be removed from the “Just Accepted” Web site and published as an ASAP article. Note that technical editing may introduce minor changes to the manuscript text and/or graphics which could affect content, and all legal disclaimers and ethical guidelines that apply to the journal pertain. ACS cannot be held responsible for errors or consequences arising from the use of information contained in these “Just Accepted” manuscripts.

SCHOLARONE™
Manuscripts

1
2
3
4
5
6
7
8
9
10
11
12
13
14
15
16
17
18
19
20
21
22
23
24
25
26
27
28
29
30
31
32
33
34
35
36
37
38
39
40
41
42
43
44
45
46
47
48
49
50
51
52
53
54
55
56
57
58
59
60

Potent, Orally Bioavailable and Efficacious Macrocyclic Inhibitors of Factor XIa. Discovery of Pyridine-Based Macrocycles Possessing Phenylazole Carboxamide P1 Groups

James R. Corte^{a,*}, Donald J. P. Pinto^{a,*}, Tianan Fang^a, Honey Osuna^a, Wu Yang^a, Yufeng Wang^a, Amy Lai^a, Charles G. Clark^a, Jung-Hui Sun^b, Richard Rampulla^b, Arvind Mathur^b, Mahammed Kaspady^c, Premsai Rai Neithnadka^c, Yi-Xin Cindy Li^a, Karen A. Rossi^a, Joseph E. Myers Jr.^b, Steven Sheriff^b, Zhen Lou^d, Timothy W. Harper^d, Christine Huang^d, Joanna J. Zheng^d, Jeffrey M. Bozarth^d, Yiming Wu^d, Pancras C. Wong^d, Earl J. Crain^d, Dietmar A. Seiffert^d, Joseph M. Luetgen^d, Patrick Y. S. Lam^a, Ruth R. Wexler^a and William R. Ewing^a

^aBristol-Myers Squibb Company, Research and Development, 350 Carter Road, Hopewell, New Jersey 08540, United States

^bBristol-Myers Squibb Company, Research and Development, US Rt. 206 & Province Line Road, Princeton, New Jersey 08540, United States

^cBristol-Myers Squibb Research Center, Syngene International Pvt. Ltd., Biocon Park, Plot No. 2 & 3, Bommasandra–Jigani Road, Bangalore 560 100, India

^dBristol-Myers Squibb Company, Research and Development, 311 Pennington-Rocky Hill Road, Pennington, New Jersey 08543, United States

KEYWORDS. Factor XIa; FXIa; Factor XIa Inhibitors; FXIa Inhibitors; Thrombosis; Activated Partial Thromboplastin Time; aPTT; Macrocycle; Anticoagulant; Antithrombotic.

ABSTRACT

Factor XIa inhibitors are promising novel anticoagulants which show excellent efficacy in preclinical thrombosis models with minimal effects on hemostasis. The discovery of potent and selective FXIa inhibitors which are also orally bioavailable has been a challenge. Here, we describe optimization of the imidazole-based macrocyclic series and our initial progress towards meeting this challenge. A two-pronged strategy, which focused on replacement of the imidazole scaffold and the design of new P1 groups, led to the discovery of potent, orally bioavailable pyridine-based macrocyclic FXIa inhibitors. Moreover, pyridine-based macrocycle **19**, possessing the phenylimidazole carboxamide P1, exhibited excellent selectivity against relevant blood coagulation enzymes and displayed antithrombotic efficacy in a rabbit thrombosis model.

* Corresponding author. Tel.: +1-609-466-5030; fax: +1-609-818-3331; e-mail: james.corte@bms.com

* Corresponding author. Tel.: +1-609-466-5068; fax: +1-609-818-3331; e-mail: donald.pinto@bms.com

INTRODUCTION

Morbidity and mortality as a result of thrombosis continues to be an area of unmet medical need.¹ Significant advances have been made by the introduction of novel oral anticoagulants that target key serine proteases in the blood coagulation cascade such as thrombin (e.g. dabigatran) or factor Xa (FXa, apixaban, rivaroxaban, edoxaban and betrixaban).²⁻³ The risk of bleeding remains a concern for all anticoagulants.⁴ Factor XIa (FXIa), another critical serine protease in the blood coagulation cascade, has emerged as an attractive target for the prevention and treatment of thrombosis with the potential of reducing the bleeding risk, thus leading to an even safer anticoagulant.⁵

Factor XIa (FXIa), the activated form of the zymogen factor XI (FXI), amplifies the generation of thrombin, the last enzyme in the blood coagulation cascade that leads to fibrin clot formation. Humans with a genetic deficiency in FXI (hemophilia C) display a minor bleeding tendency even though they show a prolongation in clotting time in the activated partial thromboplastin time (aPTT) clotting assay.⁶ Epidemiological studies revealed that individuals with a severe FXI deficiency have a lower risk of ischemic stroke and deep vein thrombosis (DVT).⁷⁻⁹ On the contrary, elevated levels of FXI are a risk factor for DVT and myocardial infarction.¹⁰⁻¹¹ Based on this evidence, it is hypothesized that inhibition of either FXI or FXIa can reduce thrombosis and preserve hemostasis thus reducing the risk of bleeding that is seen with other anticoagulants.¹²

Multiple studies have shown that therapeutic inhibition of either FXI [antisense oligonucleotides (ASO)¹³⁻¹⁴ or neutralizing antibodies¹⁵⁻¹⁷] or FXIa (irreversible¹⁸⁻²⁰ and reversible²¹⁻²⁵ small molecule inhibitors) provides antithrombotic efficacy with a low risk of

1
2
3 bleeding in a variety of preclinical animal thrombosis models. During the course of our
4
5 preclinical FXIa program, a FXI-ASO entered the clinic and provided a proof-of-concept for
6
7 targeting this key coagulation enzyme. Specifically, in a Phase II clinical trial in total knee
8
9 arthroplasty, ASO IONIS-FXIRx was shown to be superior to enoxaparin in reducing the
10
11 incidence of DVT.²⁶ In addition, the rate of clinically relevant bleeding was similar between the
12
13 IONIS-FXIRx and enoxaparin treatment arms.²⁷ A number of monoclonal antibodies (BAY
14
15 1213790,²⁸ Xisomab 3G3,²⁹ and MAA-868³⁰), as well as, small molecule FXIa inhibitors (BMS-
16
17 962212³¹ and EP-7041³²) have also entered clinical trials. However, all of these clinical agents
18
19 require a parenteral route of administration. Orally administered anticoagulants are highly
20
21 desirable especially for treating chronic thromboembolic diseases. Despite significant effort, the
22
23 discovery of potent, selective, and orally bioavailable FXIa inhibitors has been a challenge until
24
25 recently.⁵
26
27
28
29
30

31
32 We have previously reported on the discovery of a novel series of potent imidazole-based
33
34 macrocyclic FXIa inhibitors represented by 12-membered macrocycle **1** (Figure 1).³³ Despite the
35
36 excellent FXIa affinity (FXIa $K_i = 1.0$ nM) and potent in vitro anticoagulant activity as measured
37
38 by the aPTT clotting assay³⁴ ($EC_{1.5x} = 0.30$ μ M), macrocycle **1** was not orally bioavailable ($F_{rat} =$
39
40 0%). In replacing the chlorophenyltetrazole cinnamide P1 with either a benzamide P1 or cyclic
41
42 carbamate P1, we were able to reduce the polar surface area (PSA)³⁵ and improve the oral
43
44 bioavailability for 13-membered macrocycles **2** ($F_{rat} = 41\%$) and **3** ($F_{rat} = 59\%$).³⁶⁻³⁷ Despite the
45
46 good oral bioavailability, these P1 modifications led to an unacceptable loss in both FXIa affinity
47
48 and aPTT potency, as well as, poor metabolic stability in human liver microsomes ($T_{1/2} = 17$
49
50 min) and poor permeability in the Caco-2 assay (Caco-2 A to B < 15 nm/sec with a high efflux
51
52
53
54
55
56
57
58
59
60

ratio) for compound **2**.³⁸ Discovering potent, orally bioavailable FXIa inhibitors which possess good ADME properties remained as our goal.

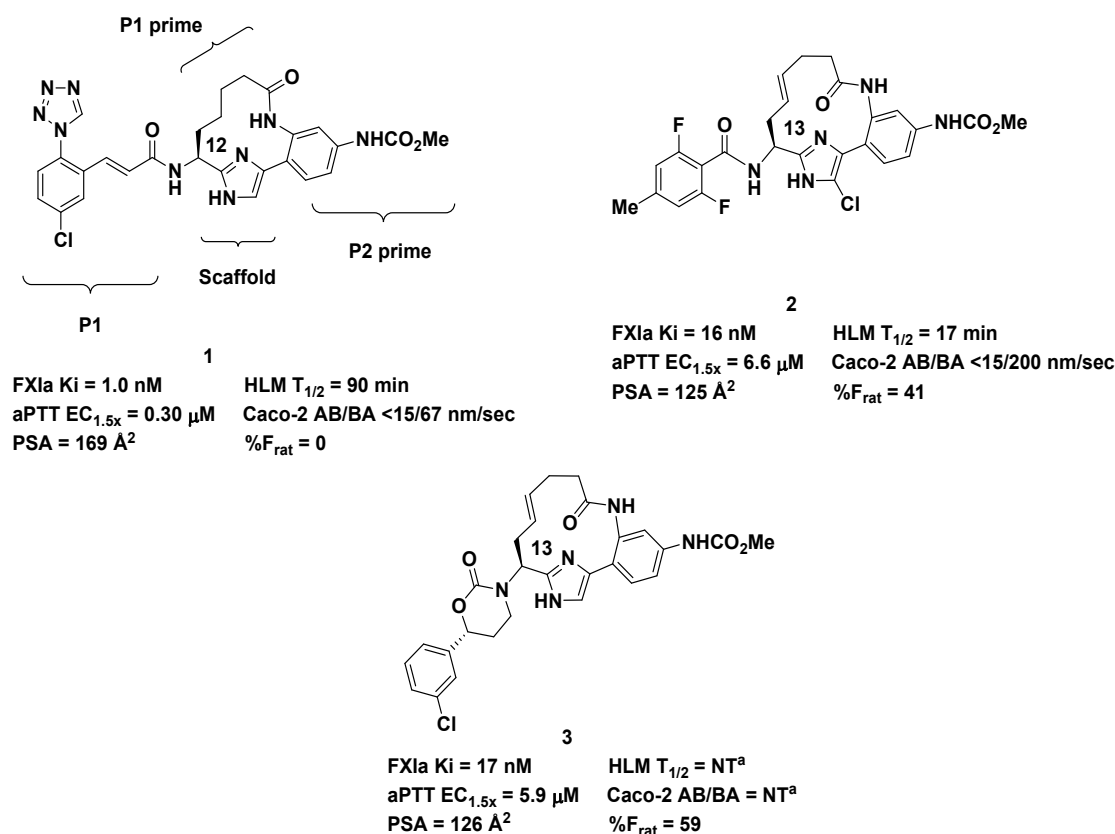


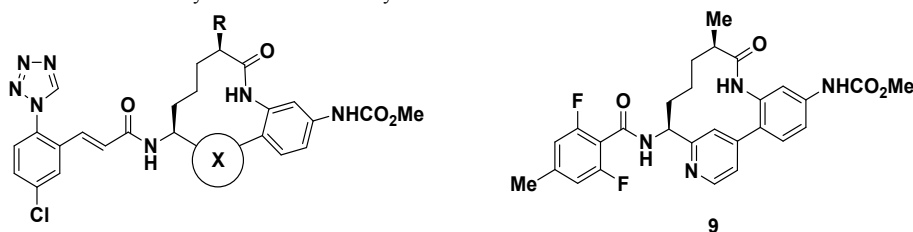
Figure 1. Imidazole-based 12- and 13-membered macrocyclic FXIa inhibitors discovered at Bristol-Myers Squibb. ^aNT = not tested.

Herein, we describe our initial progress toward achieving this goal by following a two-pronged optimization strategy that focused on 1) replacement of the imidazole scaffold and 2) design of new P1 groups. These efforts culminated in the discovery of pyridine-based macrocycles possessing novel phenylazole carboxamide P1 groups.³⁹⁻⁴⁰ Specifically, pyridine-based macrocycle **19** is a potent, orally bioavailable FXIa inhibitor that exhibited good in vitro ADME properties, excellent selectivity against relevant blood coagulation enzymes, and was efficacious in a rabbit model of arterial thrombosis.

RESULTS AND DISCUSSION

We had previously disclosed the evolution of our FXIa inhibitors from the acyclic phenyl imidazole series to the novel imidazole-based macrocyclic series.³³ Earlier, we had shown that oral bioavailability could be achieved in the acyclic phenyl imidazole series by replacing the imidazole scaffold with various 6-membered ring heterocycles.⁴¹ Based on these findings, we reasoned that replacing the imidazole scaffold in the macrocyclic series with a pyridine ring also had the potential to lead to potent FXIa inhibitors with improved oral bioavailability. To test this proposal, several key pyridine-based 12-membered macrocycles were explored (Table 1). The corresponding imidazole-based macrocycles (**1**, **4**, and **5**) which were disclosed previously are included for comparison.^{33, 36}

Table 1. 12-Membered Imidazole- and Pyridine-Based Macrocycles



Entry	X	R	FXIa Ki ^a (nM)	aPTT ^b EC _{1.5x} (μM)	HLM ^c T _{1/2} (min)	PSA (Å ²)	Caco-2 AB/BA (nm/sec)
1		H	1.0	0.33	90	169	<15/67 ^d
4		Me	0.39	0.39	NT ^e	169	NT ^e
5		Et	0.18	0.52	32	169	<15/70 ^d
6		H	1.2	0.60	40	153	<15/76 ^d
7		Me	0.18	0.62	39	153	38/66
8		Et	0.20	0.47	40	153	<15/84
9	--	--	45	27	24	109	<15/331

^aKi values were obtained from purified human enzyme at 37 °C and were averaged from multiple determinations (n ≥ 2). ^baPTT (activated partial thromboplastin time) in vitro clotting assay was performed in human plasma. EC_{1.5x} refers to the plasma concentration, not the final concentration after the addition of aPTT reagent and calcium. ^cHLM = human liver microsome stability. ^dPoor recovery in the Caco-2 permeability assay. ^eNT = Not tested.

1
2
3 Pyridine-based macrocycle **6** displayed excellent FXIa binding affinity (FXIa $K_i = 1.2$
4 nM) and potent anticoagulant activity (aPTT $EC_{1.5x} = 0.60 \mu\text{M}$) which compared favorably to
5 imidazole-based macrocycle **1**. The change in scaffold led to a modest reduction in PSA (PSA =
6 153 \AA^2 for **6** vs PSA = 169 \AA^2 for **1**), but this did not improve permeability in the Caco-2 assay.
7
8 As we reported previously, alkyl groups on the macrocyclic linker, represented in imidazole-
9 based macrocycles **4** and **5**, increased FXIa binding affinity by interacting with a lipophilic
10 region in the S1 prime (S1') pocket.³⁶ Therefore, incorporation of a methyl moiety in the
11 macrocyclic linker of the pyridine-based macrocycle led to **7** which resulted in a 6-fold
12 improvement in FXIa affinity (FXIa $K_i = 0.18 \text{ nM}$) and maintained the good anticoagulant
13 activity in the aPTT clotting assay ($EC_{1.5x} = 0.62 \mu\text{M}$). Larger alkyl groups on the macrocyclic
14 linker in the pyridine-based macrocycles did not lead to additional improvements in FXIa
15 affinity, as the ethyl substituted linker **8** was equipotent with the methyl substituted linker **7**.
16
17 Pyridine-based macrocycles **7** and **8** and imidazole-based macrocycle **5** were equipotent and
18 showed similar metabolic stability in human liver microsomes. Encouraged by the measurable
19 but low permeability in the Caco-2 assay, macrocycle **7** was evaluated in a rat pharmacokinetic
20 (PK) study (Table 5). Macrocycle **7** exhibited a low clearance, moderate volume of distribution,
21 and a long half-life but unfortunately oral exposure in rat was negligible. As the result, replacing
22 the imidazole scaffold with a pyridine ring, while maintaining excellent FXIa binding affinity
23 and potent in vitro anticoagulant activity in the aPTT clotting assay, did not improve the oral
24 bioavailability for the macrocyclic series. Next, the chlorophenyltetrazole cinnamide P1 was
25 replaced with the benzamide P1 which afforded **9**. As with the imidazole-based macrocycles,
26 incorporation of the benzamide P1 in **9** led to a significant loss in FXIa affinity (250-fold loss),
27 aPTT potency (43-fold loss), and metabolic stability with no improvement in permeability
28
29
30
31
32
33
34
35
36
37
38
39
40
41
42
43
44
45
46
47
48
49
50
51
52
53
54
55
56
57
58
59
60

(Caco-2 A to B < 15 nm/sec). At this juncture, neither the chlorophenyltetrazole cinnamide P1 nor the benzamide P1 groups were acceptable for advancement of the macrocyclic series and our focus turned to the design and discovery of new P1 groups. A new P1 group that could not only provide potent, orally bioavailable macrocycles but also maintain good ADME properties.

DESIGN AND DISCOVERY OF NEW P1 GROUPS

The design of new P1 groups was guided by a detailed analysis of the key interactions of the chlorophenyltetrazole cinnamide P1 in the S1 pocket of FXIa (Figure 2). The chlorophenyl portion fills the S1 pocket with the chlorine atom forming a π -Cl interaction with Tyr228. The tetrazole ring extends out of the S1 pocket and interacts with the Cys191-Cys219 disulfide bridge.⁴² In addition, the tetrazole N4 nitrogen forms a H-bond, via ethylene diol, to Gly216.⁴³ The cinnamide portion is in an *s-trans* orientation with the alkene twisted out of plane (60°) with the phenyl ring. The NH of the amide forms a H-bond to Ser214 via a water molecule, and the amide carbonyl interacts with the oxyanion hole and forms a H-bond with the NH of Gly193 and another H-bond with the NH of Ser195.

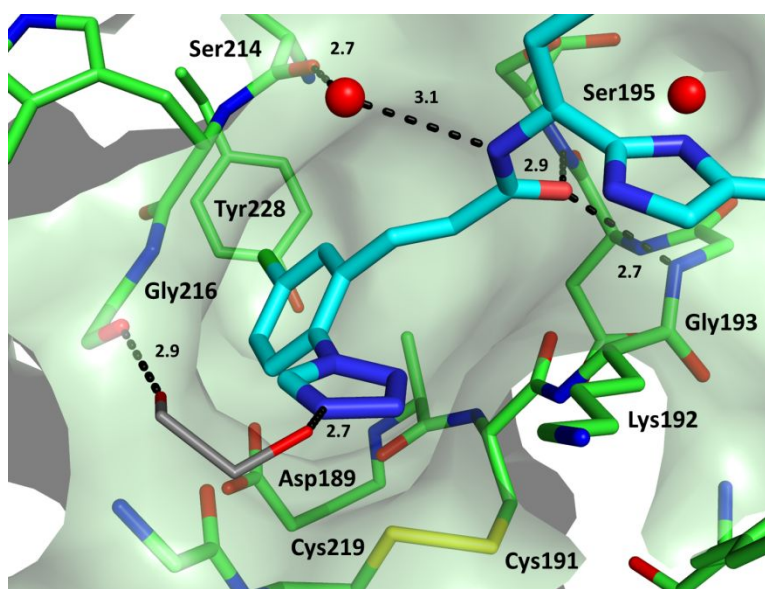


Figure 2. X-ray crystal structure of imidazole-based macrocycle **1** in Factor XIa, focusing on the key interactions of the chlorophenyltetrazole cinnamide P1 in the S1 pocket. The red spheres depict water molecules, and the dotted lines depict hydrogen bonds with distances in Angstroms. Ethylene diol is an artifact of the flash-cooling procedure.

Our strategy for modifying the chlorophenyltetrazole cinnamide and designing new P1 groups, represented by structure A, is described in Figure 3. In order to reduce PSA, the tetrazole ring was removed. Both the chlorophenyl and carboxamide groups were retained in order to preserve the key interactions with Tyr228 and the oxyanion hole, respectively. Finally, new linkers (L), which could fill the S1 pocket and have the potential to engage additional interactions in the FXIa active site, were explored as replacements for the alkene of the cinnamide.

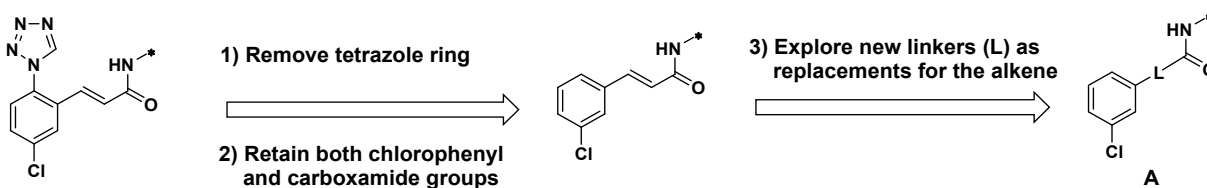
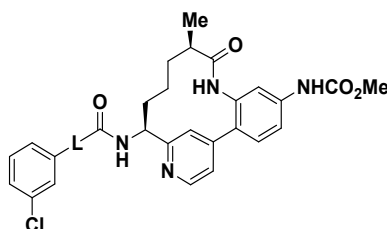


Figure 3. Strategy for designing new P1 groups.

Towards this end, a small set of saturated and unsaturated 5-membered ring heterocyclic linkers were surveyed⁴⁴ (Table 2; Note the FXIa K_i values were determined at 25 °C). Poor FXIa binding affinities were seen for pyrrolidinones **10** and **11**, as well as, pyrrolidine **12**. By comparison, pyrazole linked P1 **13** was a double-digit nanomolar FXIa inhibitor (FXIa K_i = 47 nM @ 25 °C). The FXIa K_i was also determined at 37 °C (FXIa K_i = 166 nM) for comparison with subsequent analogs.⁴⁵ The FXIa binding affinity of **13** was encouraging and it indicated that an unsaturated, five-membered ring heterocycle could serve as a suitable replacement for the alkene linker of the cinnamide.

Table 2. Survey of 5-Membered Ring P1 Linkers in Pyridine-Based Macrocycles

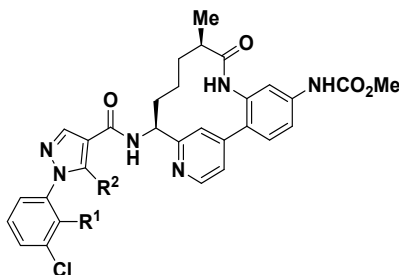
Entry	L	FXIa Ki ^a (nM)
10 (diastereomer A)		>13,000
11 (diastereomer B)		1,390
12 (diastereomeric mixture)		2,890
13		47 (166) ^b

^aKi values were obtained from purified human enzyme at 25 °C and were averaged from multiple determinations (n ≥ 2). ^bKi value was obtained at 37 °C and were averaged from multiple determinations (n ≥ 2).

To identify areas on the phenylpyrazole carboxamide P1 that could impact FXIa affinity, additional substitutions were explored (Table 3). As previously shown, the addition of a fluorine adjacent to the chlorine on the phenyl ring had provided a 2- to 8-fold improvement in FXIa affinity.^{25, 37, 46} In this case, incorporation of a fluorine group adjacent to the chlorine in the phenylpyrazole carboxamide P1 resulted in a dramatic (30-fold) increase in FXIa affinity. For example, compound **14** was a single-digit nanomolar FXIa inhibitor (FXIa Ki = 5.5 nM) and it also displayed good metabolic stability (HLM T_{1/2} = 59 min) and good permeability in the Caco-2 assay [Caco-2 AB/BA = 89/561 nm/sec; efflux ratio = 6.3]. The replacement of the fluorine with a chlorine as in **15**, led to a loss in FXIa affinity compared to **14**. Substitution on the pyrazole ring was explored next. The introduction of an amino group at the C5-position of the pyrazole (**16**) resulted in a 15-fold improvement in FXIa affinity compared to **13**. Combining the

ortho fluoro and the amino pyrazole groups in **17** led to a similar FXIa binding affinity (FXIa K_i = 3.4 nM) with a significant 6-fold increase in aPTT potency (aPTT $EC_{1.5x}$ = 1.2 μ M) observed. Importantly, **17** showed both good Caco-2 permeability, with a low efflux ratio of 4, and HLM stability.

Table 3. Phenylpyrazole Carboxamide P1 Groups in Pyridine-Based Macrocycles

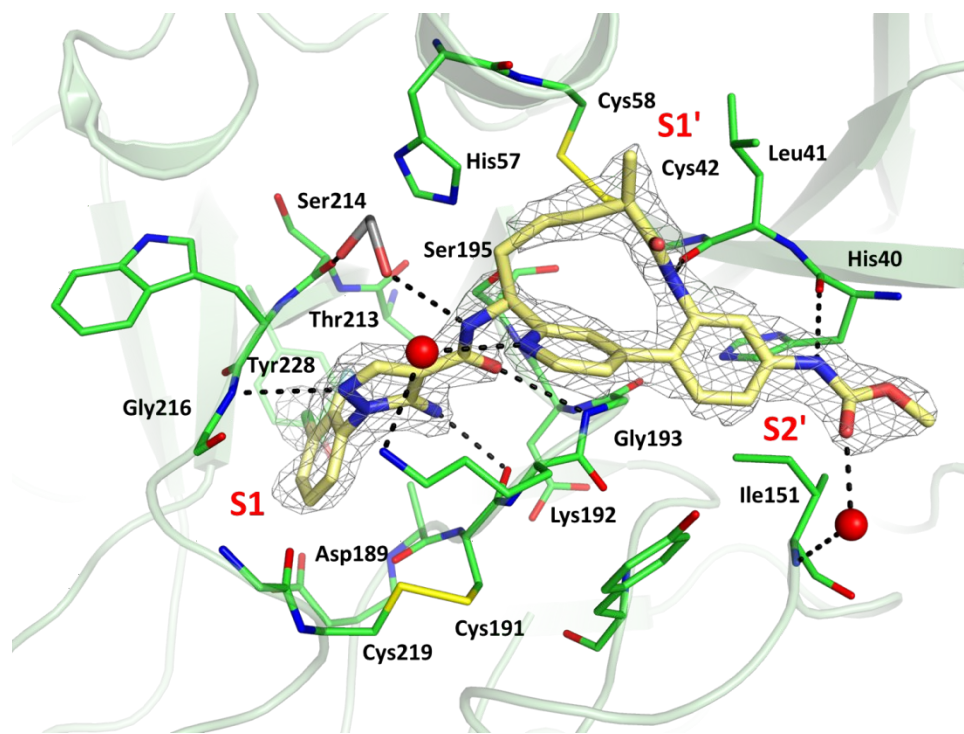


Entry	R ¹	R ²	FXIa K_i^a (nM)	aPTT ^b $EC_{1.5x}$ (μ M)	HLM ^c $T_{1/2}$ (min)	PSA (\AA^2)	Caco-2 AB/BA (nm/sec) [ER] ^d
13	H	H	166	NT ^e	NT ^e	127	NT ^e
14	F	H	5.5	7.9	59	127	89/561 [6.3]
15	Cl	H	38	>40	NT ^e	127	NT ^e
16	H	NH ₂	11	4.8	97	153	<15/134 ^f [>9]
17	F	NH ₂	3.4	1.2	50	153	40/161 [4.0]

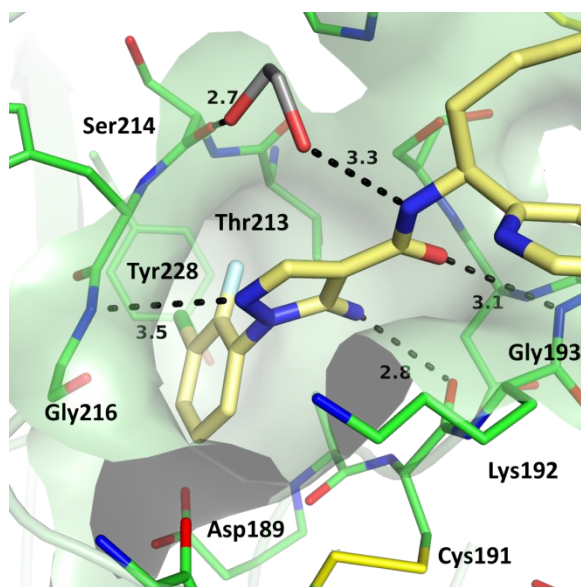
^a K_i values were obtained from purified human enzyme at 37 °C and were averaged from multiple determinations ($n \geq 2$). ^baPTT (activated partial thromboplastin time) in vitro clotting assay was performed in human plasma. $EC_{1.5x}$ refers to the plasma concentration, not the final concentration after the addition of aPTT reagent and calcium. ^cHLM = human liver microsome stability. ^dER = efflux ratio. ^eNT = Not tested. ^fPoor recovery in the Caco-2 permeability assay.

An X-ray crystal structure of **17** bound to FXIa (2.23 \AA resolution, R-work was 0.185 and R-free was 0.226, Figure 4A) was obtained and the ligand occupies the S1, S1', and S2 prime (S2') binding pockets. The macrocyclic linker fills the S1' region with the methyl substituent interacting with a lipophilic pocket. The amide NH in the macrocyclic linker forms a H-bond with the carbonyl of Leu41 (2.9 \AA). The methyl *N*-phenyl carbamate occupies the S2'

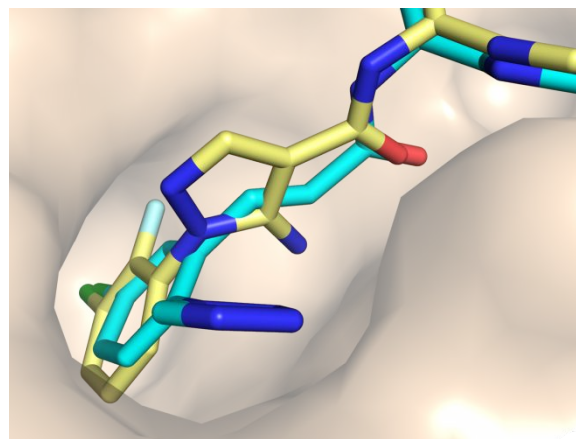
1
2
3 pocket. The NH of the carbamate forms a H-bond with the carbonyl of His40 (2.9 Å) and the
4
5 carbonyl of the carbamate forms a H-bond through a water molecule to Ile151 (2.6 Å, 3.0 Å
6
7 respectively). The pyridine nitrogen in the scaffold forms a H-bond via a water molecule to the
8
9 NH₂ of Lys192 (3.0 Å, 3.0 Å respectively). Figure 4B highlights the key interactions of the
10
11 phenylpyrazole carboxamide P1 in the S1 pocket. The chlorophenyl maintains the π -Cl
12
13 interaction with Tyr228. The ortho fluoro, which led to a significant increase in FXIa affinity in
14
15 comparing **13** and **14**, makes van der Waals contact with the side chain of Thr213. The pyrazole
16
17 ring is twisted 80° out of plane with the phenyl ring. This large dihedral angle is due to both the
18
19 steric clash between the ortho fluoro on the phenyl and the C5-NH₂ group on the pyrazole, as
20
21 well as, electrostatic repulsion between the ortho fluoro and the lone pair of the pyrazole N2. The
22
23 pyrazole N2 forms a long H-bond to Gly216 (3.5 Å), and the C5-NH₂ on the pyrazole forms a H-
24
25 bond to the carbonyl of Cys191 (2.8 Å). The NH of the carboxamide forms a H-bond to Ser214
26
27 via ethylene diol (3.3 Å, 2.7 Å respectively) and the amide carbonyl forms a H-bond with only
28
29 the NH of Gly193 (3.0 Å) in the oxyanion hole. This is in contrast to the chlorophenyltetrazole
30
31 cinnamide P1 (vide supra), where the carbonyl of the amide interacts with both Gly193 and
32
33 Ser195. An overlay of the phenylpyrazole carboxamide P1 in **17** and the chlorophenyltetrazole
34
35 P1 in **1** is provided in Figure 4C and highlights a similar trajectory for the different P1 groups
36
37 (see Supporting Information for an overlay of the entire molecules of both **17** and **1**).
38
39
40
41
42
43
44
45
46
47
48
49
50
51
52
53
54
55
56
57
58
59
60



(A)



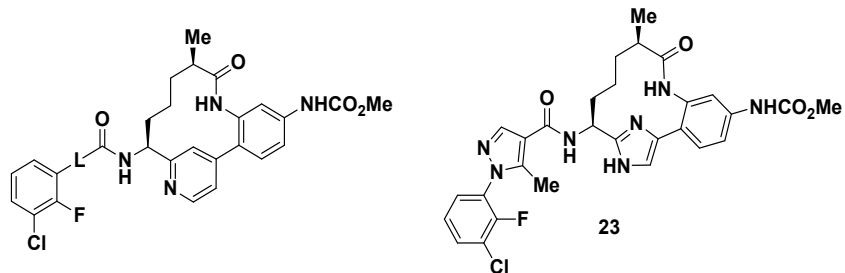
(B)



(C)

Figure 4. (A) X-ray crystal structure of **17** bound to Factor XIa with omit mFo-DFc electron density contoured at 4.0 r.m.s.d (gray). The red spheres depict water molecules, and the dotted lines depict hydrogen bonds. Ethylene diol is an artifact of the flash-cooling procedure. (B) Key interactions of the phenylpyrazole carboxamide P1 in the S1 pocket with the distances in Angstroms. (C) Overlay of phenylpyrazole carboxamide P1 (yellow) in **17** with chlorophenyltetrazole cinnamide P1 (cyan) in **1**. PDB deposition number for **17** is 5QTT.

1
2
3 Based on the X-ray crystal structure of **17**, the C5-NH₂ group on the pyrazole ring is not
4 only forming a H-bond with the carbonyl of Cys191, but it is also contributing to the large
5 dihedral angle due to the steric clash with the ortho fluoro on the phenyl ring. In order to
6 determine which is the major contributor to FXIa binding affinity, the amino was replaced with a
7 methyl group. The methyl pyrazole **18** and amino pyrazole **17** were equipotent indicating that the
8 H-bond with Cys191 had little influence on FXIa binding affinity. Importantly, replacing the C5-
9 NH₂ with the methyl group led to a reduction in PSA (PSA = 153 Å² for **17** vs PSA = 127 Å² for
10 **18**). Next we explored N-linked imidazole and triazole rings as replacements for the pyrazole
11 linker. We found that phenylimidazole carboxamide **19** showed a 2-fold loss in FXIa affinity
12 (FXIa K_i = 4.1 nM) compared to **18** but was equipotent in the in vitro clotting assay. This result
13 indicated that the H-bond between the N2 of the pyrazole in **17** (or **18**) and Gly216 (Figure 4B)
14 was not a critical interaction in the S1 pocket as **19** was devoid of this interaction. An X-ray
15 crystal structure of **19** bound to FXIa showed the phenylimidazole carboxamide P1 and the
16 phenylpyrazole carboxamide **17** bind in a very similar orientation (see Supporting Information
17 for more details). Compound **19** exhibited poor permeability in the Caco-2 assay with a high
18 efflux ratio. Phenyltriazole carboxamide **20** resulted in a 3-fold loss in both FXIa affinity and
19 aPTT clotting activity compared to **18**. C-linked phenylazoles, such as isoxazoles **21** and **22**,
20 were also explored but were less potent than the N-linked phenylazole analogs **18-20**. Having
21 discovered these new phenylazole carboxamide P1 groups, we went back and examined them in
22 the imidazole-based macrocycle and **23** is provided as a representative example. In general,
23 imidazole-based macrocycles were comparable to the corresponding pyridine-based analogs in
24 terms of FXIa affinity, aPTT potency and Caco-2 permeability but suffered from poor metabolic
25 stability in cynomolgus liver microsomes (CLM T_{1/2} ≤ 17 min).
26
27
28
29
30
31
32
33
34
35
36
37
38
39
40
41
42
43
44
45
46
47
48
49
50
51
52
53
54
55
56
57
58
59
60

Table 4. Phenylazole Carboxamide P1 Groups in Pyridine- and Imidazole-Based Macrocycles

Entry	L	FXIa Ki ^a (nM)	aPTT ^b EC _{1.5x} (μM)	LM ^c T _{1/2} H, R, D, C (min)	PSA (Å ²)	Caco-2 AB/BA (nm/sec) [ER] ^d
18		2.2	1.4	81, >120, >120, 54	127	22/348 [16]
19		4.1	2.0	55, 68, 73, 48	127	<15/367 [>24]
20		7.0	4.4	>120, >120, 118, 75	140	37/338 [9]
21		34	NT ^e	NT ^e	135	NT ^e
22		231	NT ^e	NT ^e	135	NT ^e
23	--	2.1	1.6	66, 26, 56, 17	143	37/441 [12]

^aKi values were obtained from purified human enzyme at 37 °C and were averaged from multiple determinations (n ≥ 2). ^baPTT (activated partial thromboplastin time) in vitro clotting assay was performed in human plasma. EC_{1.5x} refers to the plasma concentration, not the final concentration after the addition of aPTT reagent and calcium. ^cLM = liver microsome stability; H = human; R = rat; D = dog; C = cyno. ^dER = efflux ratio. ^eNT = Not tested.

Pharmacokinetic Profiles.

The PK profile for several macrocyclic compounds were evaluated in rat, using a discrete dosing protocol (Table 5). As mentioned earlier, **7**, a pyridine-based macrocycle containing the chlorophenyltetrazole P1, exhibited a low clearance, a long half-life but no exposure in rat. By contrast, replacing the chlorophenyltetrazole P1 with the phenylazole carboxamide P1 groups in the pyridine-based macrocycles provided moderate clearance compounds, with half-lives ranging from 1- to 2 hours, and low to modest oral bioavailability ranging from 2-42%. Interestingly, compounds **14** and **17**, which possessed good permeability with low efflux ratios, displayed poor oral exposures. On the contrary, compounds **18-20**, which possessed higher Caco-2 efflux ratios,

exhibited improved oral exposures, albeit variable upon retest (see Supporting Information for details on specific runs).⁴⁷

Table 5. Pharmacokinetic Profile In Rat For Selected Macrocycles.^a

Entry	Cl (mL/min/kg)	T _{1/2} (h)	V _{dss} (L/kg)	F (%)	AUC ^e (nM*h)	Caco-2 AB/BA (nm/sec) [ER] ^f	RLM ^g T _{1/2} (min)	Rat Protein Binding (% bound)
1	10	1.0	0.3	0	24	<15/67 [>4.5]	76	98.4
7 ^b	4.6	11.5	3.4	0	0	38/66 [1.7]	54	NT ^h
14	25	1.8	2.9	2	24	89/561 [6.3]	114	NT ^h
17	45	1.0	2.8	4	25	40/161 [4.0]	36	NT ^h
18	13-28 ^d	1.2-1.8	1.3-1.9	6-18	69-475	22/348 [16]	>120	96.7
19	6-29 ^d	1.0-1.4	0.5-2.0	7-25	68-1231	<15/367 [>24]	68	97.4
20 ^c	9-21 ^d	2.2-4.2	2.1-3.5	13-42	213-1150	37/338 [9]	>120	94.8

^aCompounds were dosed as TFA salts in rat in a discrete format. Dose: 0.70 mpk for iv arm and 1.40 mpk for po arm. Vehicle for both iv and po: 70% polypropylene glycol; 20% water; 10% ethanol. ^bDose: 0.50 mpk for iv arm and 1.0 mpk for po arm. Vehicle for both iv and po: 70% PEG-400; 20% water; 10% ethanol. ^cDose: 0.55 mpk for iv arm and 1.10 mpk for po arm. ^dThe compound was evaluated in three separate PK studies and the ranges are given here, please see Supporting Information for data on the individual runs. ^eOral AUC. ^fER= efflux ratio. ^gRLM = rat liver microsome stability. ^hNT = Not tested. Note: Compound **1** was evaluated in an n-in-1 study. Dose: 1.13 mpk for iv arm and 2.27 mpk for po arm. Vehicle for both iv and po: 70% PEG-400; 20% water; 10% ethanol.

Pyridine-based macrocycles **18-20** were also evaluated in dog and cynomolgus PK studies (Table 6). The phenylpyrazole carboxamide **18** exhibited a moderate clearance and modest oral bioavailability in dog (%F = 35). Compound **18** was also a moderate clearance compound in cyno but unfortunately showed poor oral bioavailability (%F = 4). The phenylimidazole carboxamide **19** was only dosed iv in dog, but showed a similar PK profile to **18** and was a moderate clearance compound with a long half-life (T_{1/2} = 5 h) and a high volume distribution. In contrast to **18**, compound **19** displayed low clearance and modest oral bioavailability in cyno (%F = 19). The phenyltriazole carboxamide **20**, exhibited low clearance, a long half-life and modest oral bioavailability in both dog (%F = 34) and cyno (%F = 15).

Table 6. Pharmacokinetic Profile In Dog and Cyno For Pyridine-Based Macrocyces **18**, **19**, and **20**.^a

Entry	Species	Cl (mL/min/kg)	T _{1/2} (h)	V _{dss} (L/kg)	F (%)	AUC ^b (nM*h)	Dose iv/po (mpk)	LM ^c T _{1/2} (min)	Protein Binding (% bound)
18	Dog	16.4	2.9	4.0	35	266	0.40/0.57	>120	95.0
	Cyno	20	3.3	3.6	4	69	0.72/1.33	54	96.4
19	Dog	15.6	5.0	6.0	IV only	IV only	0.80/NT	73	95.7
	Cyno	14.5	3.7	3.2	19	509	0.80/1.58	48	95.8
20	Dog	5.4	4.8	2.4	34	922	0.40/0.62	118	96.2
	Cyno	9.9	4.0	2.9	15	584	0.71/1.52	75	94.5

^aCompounds were dosed as TFA salts in dog and as HCl salts in cyno in a discrete format. Vehicle for both iv and po: 70% PEG-400; 20% water; 10% ethanol. ^bOral AUC. ^cLM = liver microsome stability.

A cohort of potent, pyridine-based macrocyclic FXIa inhibitors (**18-20**) exhibiting good ADME properties and improved, yet modest, oral bioavailability had been discovered. With this achievement in hand, our focus turned to the evaluation of a pyridine-based macrocycle in a rabbit thrombosis model (vide infra). As a prelude to this efficacy study, both rabbit FXIa binding affinity and rabbit aPTT assays were measured for compounds **18-20** (Table 7). Only a 2-fold loss in binding affinity was seen in rabbit when compared to human. However, a more dramatic loss in potency in the rabbit aPTT clotting assay was seen which was presumably due to a combination of lower binding affinity and higher protein binding for rabbit compared to human. Macrocycle **19** showed the best balance of potency in both human and rabbit (Table 7) and desirable PK parameters (Tables 5 and 6). Compound **19** exhibited >600 fold selectivity against many of the relevant serine proteases (Table 8), except for plasma kallikrein (1.5-fold), with no significant inhibition (IC₅₀ > 20 μM) toward cytochrome P450 enzymes or the hERG ion channel (26% inhibition at 30 μM). As a result, **19** was selected for further evaluation in a rabbit model of arterial thrombosis.

Table 7. Comparison of Human and Rabbit In Vitro Potency for Macrocycles **18-20**.

Entry	Human FXIa Ki ^a (nM)	Rabbit FXIa Ki ^b (nM)	Human aPTT ^c EC _{1.5x} (μM)	Rabbit aPTT ^d EC _{1.5x} (μM)
18	2.2	4.6	1.4	30
19	4.1	9.6	2.0	35
20	7.0	15.2	4.4	42

^aKi values were obtained from purified human enzyme at 37 °C and were averaged from multiple determinations (n ≥ 2).

^bKi values were obtained from purified rabbit enzyme at 37 °C and were averaged from multiple determinations (n ≥ 2).

^caPTT (activated partial thromboplastin time) in vitro clotting assay was performed in human plasma.

^daPTT (activated partial thromboplastin time) in vitro clotting assay was performed in rabbit plasma. For compounds **18-20**, the rabbit free fraction is ~1% while free fraction in human plasma is 3 to 4%.

Table 8. Human Serine Protease Selectivity Profile for Compound **19**.

Human Enzyme	Ki (nM) ^a	Selectivity (fold)
Factor XIa	4.1	NA^c
Factor VIIa^b	>13,300	>3,100
Factor IXa	>27,100	>6,600
Factor Xa	>13,300	>3,100
Factor XIIa	2,530	620
Thrombin	>11,500	>2,800
Trypsin	>10,000	>2,400
Plasma Kallikrein	6.3	1.5
Activated Protein C	>21,500	>5,200
Plasmin	>15,000	>3,600
TPA	2,940	720
Urokinase	>15,100	>3,600

^aKi values in nM were obtained using human purified enzymes at 37 °C.

^bFVIIa Ki values in nM were obtained using human purified enzyme at 25 °C, please see experimental section for details.

^cNA = Not applicable.

RABBIT ECAT EFFICACY MODEL

The rabbit electrically induced carotid arterial thrombosis (ECAT) model has been used to evaluate a number of marketed anticoagulants (warfarin, dabigatran, and apixaban) and antiplatelet agents (clopidogrel and prasugrel).^{22, 48-49} In this model, thrombosis was induced by electrical stimulation and carotid blood flow was measured to monitor thrombosis-induced

occlusion. Compound **19** was evaluated in this model and produced a dose-dependent increase in blood flow of the injured carotid artery (Figure 5A). In addition, a dose-dependent reduction in thrombus formation was demonstrated with an estimated ED₅₀ of 1.6 mg/kg + 1 mg/kg/h (Figure 5B).

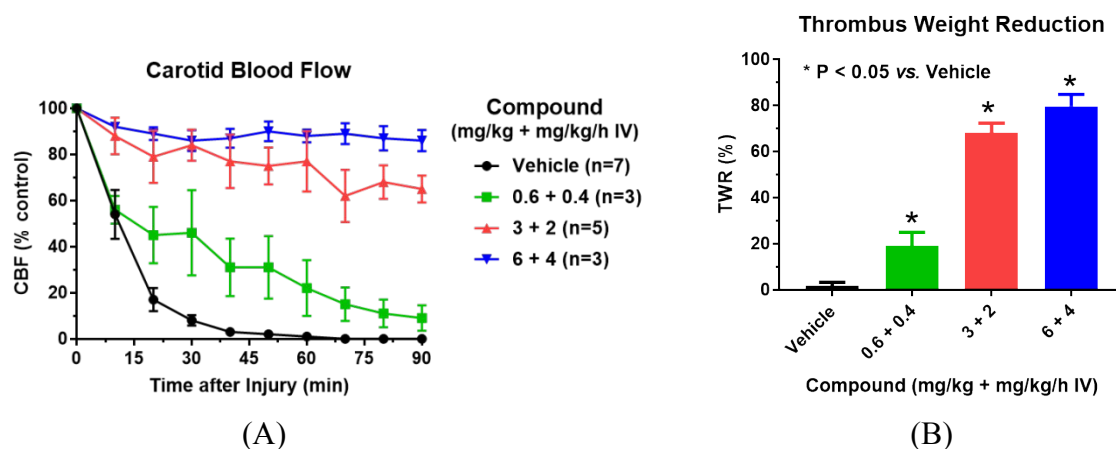


Figure 5. Antithrombotic effect of compound **19** in rabbit ECAT model. (A) Carotid blood flow versus time following arterial injury. CBF = carotid blood flow. (B) Antithrombotic dose-response. TWR = thrombus weight reduction. Vehicle = 10% dimethylacetamide : 90% cyclodextrin.

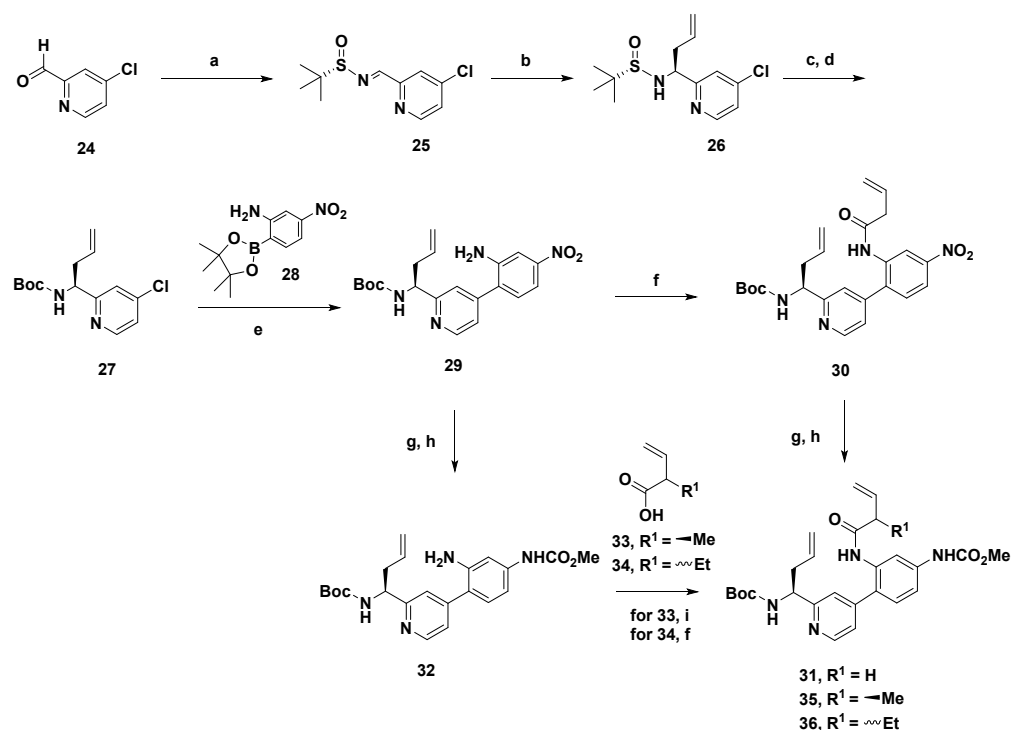
CHEMISTRY

A ring-closing olefin (RCM) metathesis strategy was employed as the key step in the synthesis for both the pyridine- and imidazole-based macrocycles.⁵⁰ The preparation of the RCM precursors for the 12-membered pyridine-based macrocycles is described in Scheme 1.

Condensation of aldehyde **24**⁵¹ with (*S*)-2-methylpropane-2-sulfinamide in the presence of anhydrous CuSO₄ and Cs₂CO₃ afforded sulfinimine **25**. Using a modified procedure described by Sun et al.,⁵² an allylindium species, prepared by transmetalation of allylmagnesium bromide with indium(III) chloride, was added to sulfinimine **25**, which gave sulfinamide **26** with excellent diastereoselectivity (>19:1 diastereomeric excess).^{53,54} Protecting group interconversion

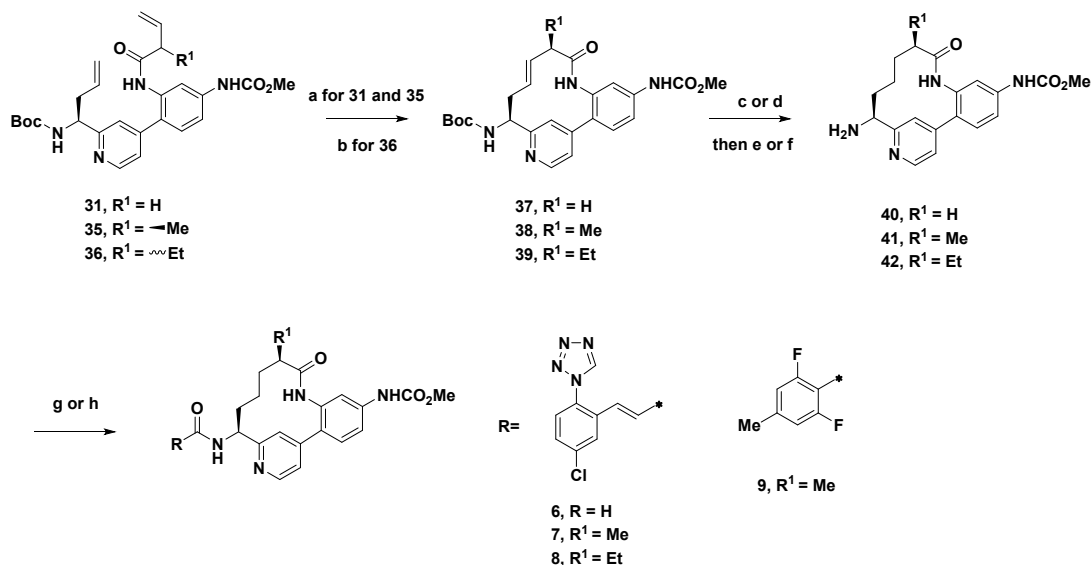
was accomplished in two steps to give **27**. Suzuki-Miyaura coupling between 4-chloropyridine **27** and boronic ester **28** provided aniline **29**. Aniline **29** was coupled with 3-butenic acid using T₃P and DIPEA which gave diene **30**. Reduction of the nitro to the aniline intermediate followed by reaction with methyl chloroformate afforded RCM precursor **31**. An alternative sequence was used to prepare RCM precursors **35** and **36**. Reduction of the nitro to the *bis*-aniline intermediate and selective introduction of the carbamate at -78 °C gave aniline **32**. Aniline **32** was then coupled with (*R*)-2-methylbut-3-enoic acid (**33**) using T₃P and pyridine which gave **35**. The choice of pyridine base was critical in preventing epimerization in the amide coupling step with chiral acid **33**. Aniline **32** was also coupled with (±)-2-ethylbut-3-enoic acid (**34**) that gave RCM precursor **36** as a mixture of diastereomers.

Scheme 1. Synthesis of RCM Precursors for the Pyridine-Based Macrocycles.^a



The synthesis of the pyridine-based 12-membered macrocycles possessing the chlorophenyltetrazole and benzamide P1 groups is described in Scheme 2. RCM precursors **31** and **35** were treated with *p*TsOH to form the pyridinium salt and then cyclized at 40 °C using Grubbs (II) catalyst which provided macrocycles **37** and **38**.⁵⁵ A modified procedure was used for the macrocyclization of **36**. RCM precursor **36** was subjected to Grubbs (II) catalyst in a microwave at 120 °C, followed by separation of diastereomers by normal phase chromatography, afforded macrocycle **39**. Hydrogenation of **37-39** over palladium on carbon, followed by deprotection with either TFA or 4M HCl in dioxane yielded the saturated macrocyclic amines **40-42**. The macrocyclic amines **40-42** were coupled with (*E*)-2,5-dioxopyrrolidin-1-yl 3-(5-chloro-2-(1H-tetrazol-1-yl)phenyl)acrylate⁴¹ or 2,6-difluoro-4-methylbenzoic acid, which gave the corresponding amides **6-9**.

Scheme 2. Synthesis of Pyridine-Based Macrocycles **6-9** from Table 1.^a

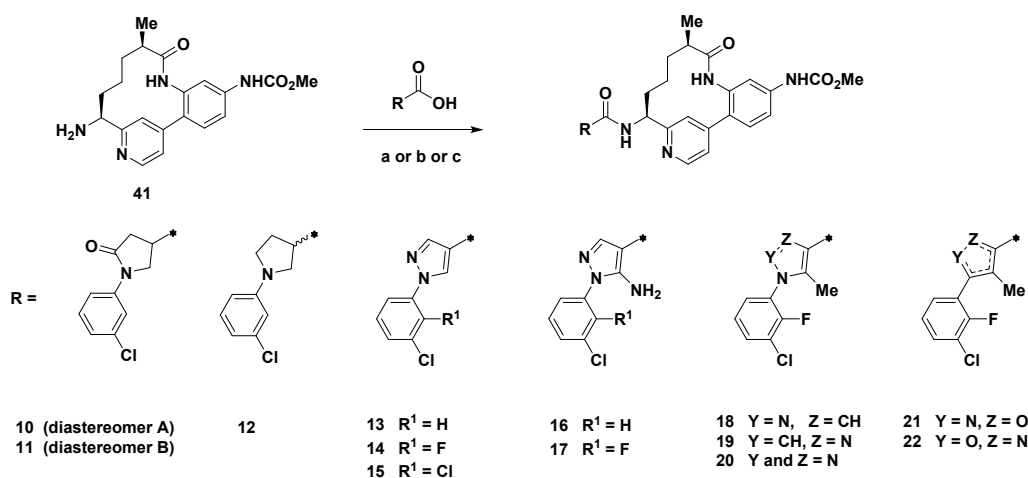


^aReagents and conditions: (a) Grubbs II catalyst (20 mol%), *p*TsOH-H₂O, DCM, reflux, for **37**: 53%, for **38**: 73%; (b) Grubbs II catalyst (20 mol%), DCE, microwave, 120 °C, diastereomers were separated by normal phase chromatography, 16%; (c) 10% Pd/C, H₂, MeOH, 100%; (d) 10% Pd/C, H₂ (55 psi), MeOH, THF, 90%; (e) 4M HCl

in dioxane, 90%; (f) TFA, DCM, 100%; (g) (*E*)-2,5-dioxopyrrolidin-1-yl 3-(5-chloro-2-(1H-tetrazol-1-yl)phenyl)acrylate, DIPEA, DMF, 41-74% (h) 2,6-difluoro-4-methylbenzoic acid, EDC, HOBt, DIPEA, DMF, 58%.

Scheme 3 describes the syntheses of the pyridine-based macrocycles **10-22** from Tables 2, 3 and 4. Macroyclic amine **41** was coupled with the various phenylpyrrolidinone-, phenylpyrrolidine- and phenylazole carboxylic acids, which afforded analogs **10-22**. The synthesis of the imidazole-based macrocycle **23** followed a similar sequence as described for the pyridine-based macrocycles (see Supplemental Information Scheme S1).

Scheme 3. Synthesis of Pyridine-Based Macrocycles **10-22** in Tables 2, 3 and 4.^a

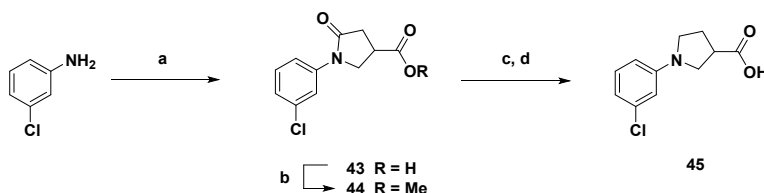


^aReagents and conditions: (a) phenylpyrrolidinone carboxylic acid **43**, phenylpyrrolidine carboxylic acid **45**, or phenylazole carboxylic acid **48a** and **48c-d**, EDC, HOBt, TEA, DMF, 50 °C, 17-55%; (b) phenylazole carboxylic acids **48b**, **48e**, **50**, **52**, **54**, or **57**, EDC, HOBt, DIPEA, DMF, rt, 28-77%; (c) phenylisoxazole carboxylic acid **60**, EDC, HOBt, DIPEA, DMF, rt to 55 °C, 34%.

Scheme 4 describes the synthesis of phenylpyrrolidinone carboxylic acid **43** and phenylpyrrolidine carboxylic acid **45**. Condensation of 3-chloroaniline and 2-methylenesuccinic acid at elevated temperature afforded phenylpyrrolidinone carboxylic acid **43**.⁵⁶ Acid **43** was converted to the methyl ester **44**. Reduction of the lactam carbonyl with BH₃-THF complex followed by hydrolysis of the ester provided phenylpyrrolidine carboxylic acid **45**.

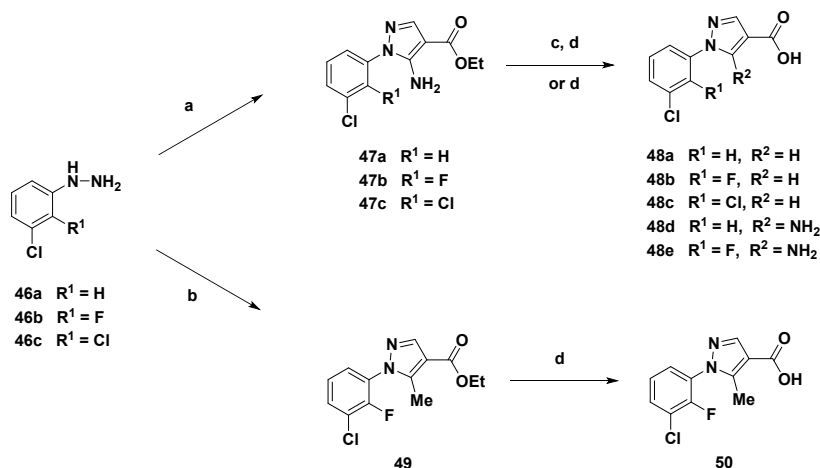
The syntheses for the phenylpyrazole carboxylic acid intermediates are described in Scheme 5. Appropriately substituted phenylhydrazines **46a-c** were condensed with (*E*)-ethyl 2-cyano-3-ethoxyacrylate, which provided aminopyrazoles **47a-c**. Treatment of **47a-c** with isoamyl nitrite in THF at elevated temperatures,⁵⁷ followed by hydrolysis of the ester, afforded the unsubstituted phenylpyrazole carboxylic acids **48a-c**. Hydrolysis of **47a** and **47b** gave C5-amino pyrazole carboxylic acids **48d** and **48e**. Phenylhydrazine **46b** was condensed with ethyl 2-((dimethylamino)methylene)-3-oxobutanoate to make C5-methyl pyrazole **49**. Hydrolysis of the ester then afforded C5-methyl pyrazole carboxylic acid **50**.

Scheme 4. Synthesis of Phenylpyrrolidinone and Phenylpyrrolidine Carboxylic Acid Intermediates.^a



^aReagents and conditions: (a) 2-methylenesuccinic acid, 120 °C, then H₂O, 110 °C, 52%; (b) SOCl₂, MeOH, rt, 0 °C to rt, 98%; (c) BH₃-THF, THF, rt, 69%; (d) NaOH (aq), MeOH, rt, 91%.

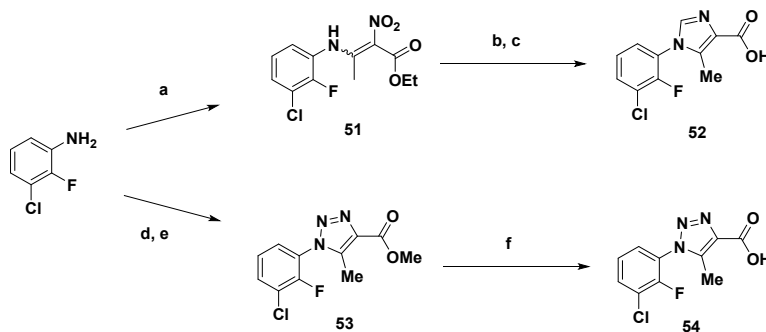
Scheme 5. Synthesis of Phenylpyrazole Carboxylic Acid Intermediates.^a



^aReagents and conditions: (a) (*E*)-ethyl 2-cyano-3-ethoxyacrylate, K₂CO₃, EtOH, reflux, 66-85%; or (*E*)-ethyl 2-cyano-3-ethoxyacrylate, NaOAc, AcOH, H₂O, rt to 100 °C, 74%; or (*E*)-ethyl 2-cyano-3-ethoxyacrylate, TEA, EtOH, reflux, 34%; (b) ethyl 2-((dimethylamino)methylene)-3-oxobutanoate, TEA, EtOH, rt, 45%; (c) isoamyl nitrite, THF, 65 °C or reflux, 80-86%; (d) NaOH, H₂O, MeOH, rt or 50 °C, 85-96%; or NaOH, H₂O, EtOH, reflux, 87-88%; or LiOH, H₂O, THF, MeOH, rt, 81%.

The syntheses for phenylimidazole carboxylic acid **52** and phenyltriazole carboxylic acid **54** are described in Scheme 6. Addition of 3-chloro-2-fluoroaniline to ethyl 3-ethoxy-2-nitrobut-2-enoate gave **51**. Reacting **51** with triethyl orthoformate and platinum on carbon under a hydrogen atmosphere at 75 °C afforded, following hydrolysis of the ester, phenylimidazole carboxylic acid **52**.⁵⁸ Diazotization of 3-chloro-2-fluoroaniline and displacement with NaN₃ provided the corresponding arylazide intermediate that was condensed with methyl acetoacetate in the presence of piperidine to give C5-methyl triazole **53**.⁵⁹ Hydrolysis of **53** afforded phenyltriazole carboxylic acid **54**.

Scheme 6. Synthesis of Phenylimidazole and Phenyltriazole Carboxylic Acid Intermediates.^a

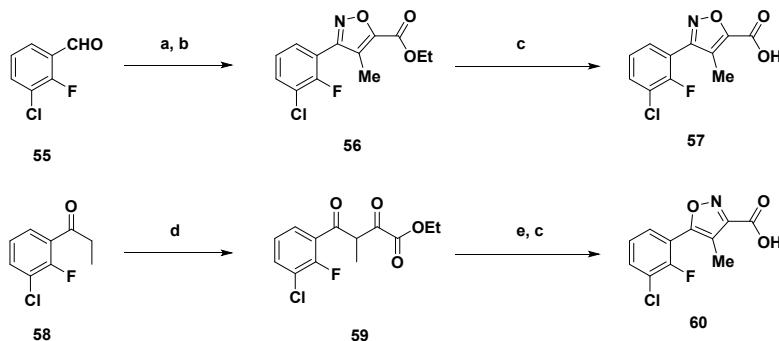


^aReagents and conditions: (a) ethyl 3-ethoxy-2-nitrobut-2-enoate, EtOH, rt, 36%; (b) 10% Pt/C, H₂ (balloon), triethyl orthoformate, 75 °C, 61%; (c) NaOH, MeOH, rt, 81%; (d) TFA, H₂O, NaNO₂, then NaN₃, 0 °C to rt; (e) methyl acetoacetate, piperidine, DMSO, H₂O, rt, 81% over two steps; (f) NaOH, MeOH, H₂O, 80 °C, 53%.

Scheme 7 describes the syntheses of the phenylisoxazole carboxylic acids **57** and **60**. Condensation of 3-chloro-2-fluorobenzaldehyde with hydroxylamine gave the corresponding 3-chloro-2-fluorobenzaldehyde oxime. Oxidation of the oxime with MagtrieveTM generated the nitrile oxide in situ which undergoes a 1,3-dipolar cycloaddition with ethyl but-2-ynoate to give isoxazole **56**.⁶⁰ Hydrolysis of **56** provided the phenylisoxazole carboxylic acid **57**. The

regioisomeric phenylisoxazole carboxylic acid **60** was prepared in three steps from ketone **58**.⁶¹ Deprotonation of ketone **58** with LiHMDS and reaction with diethyl oxalate provided diketoester **59**. Treatment of diketoester **59** with hydroxylamine led to the formation of the corresponding isoxazole and subsequent hydrolysis gave phenylisoxazole carboxylic acid **60**.

Scheme 7. Synthesis of Phenylisoxazole Carboxylic Acid Intermediates.^a



^aReagents and conditions: (a) $\text{NH}_2\text{OH}\cdot\text{HCl}$, NaOH , H_2O , EtOH , rt, 92%; (b) ethyl but-2-ynoate, MagtrieveTM, CH_3CN , $80\text{ }^\circ\text{C}$, 2%; (c) NaOH , H_2O , MeOH , rt, 100%; (d) LiHMDS , Et_2O , diethyl oxalate, $-78\text{ }^\circ\text{C}$, 6%; (e) $\text{NH}_2\text{OH}\cdot\text{HCl}$, EtOH , $90\text{ }^\circ\text{C}$, 39%.

CONCLUSION

We described the optimization of imidazole-based macrocyclic FXIa series, which focused on replacing the imidazole scaffold with a pyridine ring system as well as the design of new P1 groups. These efforts led to the discovery of potent, orally bioavailable pyridine-based macrocycles containing phenylazole carboxamide P1 groups. The pyridine-based macrocyclic series, exemplified by compound **19**, exhibited excellent selectivity against relevant blood coagulation enzymes and is the first reported macrocyclic inhibitor of FXIa to display potent antithrombotic efficacy in the rabbit ECAT model. Further optimization of the pyridine-based macrocyclic FXIa inhibitors, which led to additional improvements in oral bioavailability, will be reported in due course.

EXPERIMENTAL

General Chemistry Methods. All reactions were carried out using commercial grade reagents and solvents. Solution ratios express a volume relationship, unless stated otherwise. NMR chemical shifts (δ) are reported in parts per million relative to internal TMS, CDCl_3 , CD_3OD , or DMSO-d_6 . Normal phase chromatography was carried out on ISCO CombiFlash systems using prepacked silica cartridges and eluted with gradients of the specified solvents. Preparative reverse phase high pressure liquid chromatography (HPLC) was carried out on C18 HPLC columns using methanol/water gradients containing 0.1% trifluoroacetic acid unless otherwise stated. Purity of all final compounds was determined to be $\geq 95\%$ by analytical HPLC using the following conditions: SunFire C18 column (3.5 μm C18, 3.0 x 150 mm); Gradient elution (0.5 mL/min) from 10-100% Solvent B for 12 min and then 100% Solvent B for 3 min. Solvent A is (95% water, 5% acetonitrile, 0.05% TFA) and Solvent B is (5% water, 95% acetonitrile, 0.05% TFA); monitoring UV absorbance at 220 and 254 nm. Marvin Sketch 16.12.19 was used to name all macrocycles.

Methyl

***N*-[(14*S*)-14-[(2*E*)-3-[5-chloro-2-(1*H*-1,2,3,4-tetrazol-1-yl)phenyl]prop-2-enamido]-9-oxo-8,16-diazatricyclo[13.3.1.0^{2,7}]nonadeca-1(19),2(7),3,5,15,17-hexaen-5-yl]carbamate,**

Trifluoroacetic acid salt (6). A clear, pale pink solution of **40** (0.070 g, 0.12 mmol) and (*E*)-2,5-dioxopyrrolidin-1-yl 3-(5-chloro-2-(1*H*-tetrazol-1-yl)phenyl)acrylate⁴¹ (0.038 g, 0.11 mmol) in DMF (1.20 mL) and DIPEA (0.11 mL, 0.60 mmol) was stirred at rt for 4 h. Then, H_2O (4 mL) was added dropwise to the vigorously stirred reaction to give a suspension. The solid was

collected by filtration to give a pink solid. The cloudy filtrate was extracted with 10% IPA/CHCl₃ (3x). The combined organic layers were washed with brine and then concentrated to give a pink residue which was combined with the pink solid. Purification by reverse phase chromatography gave, following concentration and lyophilization, **6** (62.3 mg, 74%) as a pale yellow solid. MS (ESI) *m/z*: 587.3 (M+H)⁺. ¹H NMR (500 MHz, DMSO-d₆) δ 9.97 (s, 1H), 9.84 (s, 1H), 9.81 (s, 1H), 8.76 (d, *J*=6.3 Hz, 1H), 8.68 (d, *J*=5.2 Hz, 1H), 7.93 (d, *J*=1.9 Hz, 1H), 7.75 (br dd, *J*=8.5, 2.2 Hz, 1H), 7.73 - 7.70 (m, 2H), 7.56 - 7.52 (m, 2H), 7.50 (dd, *J*=8.5, 1.9 Hz, 1H), 7.39 (d, *J*=1.7 Hz, 1H), 6.95 (d, *J*=15.7 Hz, 1H), 6.84 (d, *J*=15.7 Hz, 1H), 5.06 - 4.99 (m, 1H), 3.70 (s, 3H), 2.42 - 2.35 (m, 1H), 1.96 - 1.85 (m, 1H), 1.81 - 1.64 (m, 3H), 1.58 - 1.43 (m, 1H), 1.27 - 1.11 (m, 1H), 0.65 - 0.47 (m, 1H). ¹³C NMR (126 MHz, DMSO-d₆) δ 170.6, 163.5, 158.3 (q, *J*=35.8 Hz, 1C), 156.8, 153.8, 150.3, 147.0, 145.2, 141.0, 136.2, 135.8, 133.0, 130.92, 130.86, 130.1, 129.9, 129.0, 128.4, 127.5, 126.9, 122.5 (overlap of two carbons based on HMQC), 117.0, 116.4, 115.8 (q, *J*=292.5 Hz, 1C), 52.3, 51.8, 35.9, 31.9, 22.8, 22.6.

Methyl

***N*-[(10*R*,14*S*)-14-[(2*E*)-3-[5-chloro-2-(1*H*-1,2,3,4-tetrazol-1-yl)phenyl]prop-2-enamido]-10-methyl-9-oxo-8,16-diazatricyclo[13.3.1.0^{2,7}]nonadeca-1(19),2(7),3,5,15,17-hexaen-5-yl]carbamate, Trifluoroacetic acid salt (7)**. To a solution of **41**, 2TFA (0.028 g, 0.047 mmol) in DMF (1 mL) was added (*E*)-2,5-dioxopyrrolidin-1-yl 3-(5-chloro-2-(1*H*-tetrazol-1-yl)phenyl)acrylate⁴¹ (0.016 g, 0.047 mmol) and DIPEA (0.041 mL, 0.24 mmol). The rxn was stirred at rt for 18 h. Then the reaction was diluted with MeOH and purification by reverse phase chromatography gave, following concentration and lyophilization, **7** (0.020 g, 59%) as a white solid. MS (ESI) *m/z*: 601.0 (M+H)⁺. ¹H NMR (500 MHz, CD₃OD) δ 9.66 (s, 1H, NH), 9.48 (s, 1H), 8.69 (d, *J*=6.3 Hz, 1H), 8.18 (d, *J*=1.7 Hz, 1H), 7.97 (d, *J*=2.2 Hz, 1H), 7.90 (dd, *J*=6.2, 1.8 Hz, 1H), 7.66

(dd, $J=8.5, 2.5$ Hz, 1H), 7.61 (d, $J=8.5$ Hz, 1H), 7.58 - 7.54 (m, 2H), 7.48 (dd, $J=8.5, 2.2$ Hz, 1H), 7.10 (d, $J=15.4$ Hz, 1H), 6.79 (d, $J=15.4$ Hz, 1H), 5.15 (dd, $J=11.0, 6.1$ Hz, 1H), 3.77 (s, 3H), 2.78 - 2.71 (m, 1H), 2.19 - 2.09 (m, 1H), 1.97 - 1.83 (m, 2H), 1.67 - 1.44 (m, 2H), 0.95 (d, $J=6.9$ Hz, 3H), 0.55 - 0.40 (m, 1H).

Methyl

N-[(10*R*,14*S*)-14-[(2*E*)-3-[5-chloro-2-(1*H*-1,2,3,4-tetrazol-1-yl)phenyl]prop-2-enamido]-10-ethyl-9-oxo-8,16-diazatricyclo[13.3.1.0^{2,7}]nonadeca-1(19),2(7),3,5,15,17-hexaen-5-yl]carbamate, Trifluoroacetic acid salt (8). Using a procedure analogous to that which was used to prepare **6**, compound **42** (0.010 g, 0.016 mmol) was coupled with (E)-2,5-dioxopyrrolidin-1-yl 3-(5-chloro-2-(1*H*-tetrazol-1-yl)phenyl)acrylate (5.70 mg, 0.016 mmol) to give **8** (0.0050 g, 41%) as a yellow solid. MS (ESI) m/z : 615.4 (M+H)⁺ and 617.4 (M+2+H)⁺. ¹H NMR (500 MHz, CD₃OD) δ 9.67 (s, 1H, NH), 9.49 (s, 1H), 8.69 (d, $J=6.1$ Hz, 1H), 8.14 (d, $J=1.7$ Hz, 1H), 7.97 (d, $J=2.2$ Hz, 1H), 7.88 (dd, $J=6.1, 1.9$ Hz, 1H), 7.67 (dd, $J=8.5, 2.5$ Hz, 1H), 7.62 (d, $J=8.5$ Hz, 1H), 7.59 - 7.55 (m, 2H), 7.49 (dd, $J=8.5, 2.2$ Hz, 1H), 7.10 (d, $J=15.7$ Hz, 1H), 6.78 (d, $J=15.7$ Hz, 1H), 5.13 (dd, $J=11.1, 5.9$ Hz, 1H), 3.77 (s, 3H), 2.50 - 2.43 (m, 1H), 2.20 - 2.10 (m, 1H), 1.95 - 1.78 (m, 2H), 1.67 - 1.49 (m, 2H), 1.48 - 1.38 (m, 1H), 1.31 - 1.21 (m, 1H), 0.85 (t, $J=7.3$ Hz, 3H), 0.66 - 0.54 (m, 1H).

Methyl N-[(10*R*,14*S*)-14-(2,6-difluoro-4-methylbenzamido)-10-methyl-9-oxo-8,16-diazatricyclo[13.3.1.0^{2,7}]nonadeca-1(19),2(7),3,5,15,17-hexaen-5-yl]carbamate, Trifluoroacetic acid salt (9). A clear, pink solution of **41**, 2HCl (0.015 g, 0.034 mmol), 2,6-difluoro-4-methylbenzoic acid (5.85 mg, 0.034 mmol), EDC (9.77 mg, 0.051 mmol), and HOBT (7.81 mg, 0.051 mmol) in DMF (0.34 mL) and DIPEA (0.030 mL, 0.17 mmol) was stirred at rt. After 17 h, the reaction was partitioned between EtOAc and water and the layers were separated.

The aqueous layer was extracted with EtOAc (2x). The organic layers were combined, washed with sat. NaHCO₃, brine, dried over Na₂SO₄, filtered and concentrated to give an off-white solid. The solid was dissolved in 1:1 DMF/MeOH and one drop of TFA. Purification by reverse phase chromatography gave, after concentration and lyophilization, **9** (0.0126 g, 58%) as a white solid. MS (ESI) *m/z*: 523.3 (M+H)⁺. ¹H NMR (500 MHz, CD₃OD) δ 9.65 (s, 1H, NH), 8.75 (d, *J*=6.1 Hz, 1H), 8.16 (d, *J*=1.7 Hz, 1H), 7.88 (dd, *J*=5.9, 1.8 Hz, 1H), 7.64 (d, *J*=8.5 Hz, 1H), 7.57 (d, *J*=1.9 Hz, 1H), 7.51 (dd, *J*=8.5, 2.2 Hz, 1H), 6.90 (d, *J*=8.8 Hz, 2H), 5.29 (dd, *J*=11.3, 6.1 Hz, 1H), 3.77 (s, 3H), 2.79 - 2.69 (m, 1H), 2.38 (s, 3H), 2.20 - 2.08 (m, 1H), 2.02 - 1.84 (m, 2H), 1.69 - 1.56 (m, 1H), 1.54 - 1.41 (m, 1H), 0.95 (d, *J*=6.9 Hz, 3H), 0.58 - 0.42 (m, 1H). ¹⁹F NMR (471 MHz, CD₃OD) δ -77.3, -116.2.

Methyl

***N*-[(10*R*,14*S*)-14-[1-(3-chlorophenyl)-5-oxopyrrolidine-3-amido]-10-methyl-9-oxo-8,16-diazatricyclo[13.3.1.0^{2,7}]nonadeca-1(19),2(7),3,5,15,17-hexaen-5-yl]carbamate, Trifluoroacetic acid salt (**10**, Diastereomer A) and Methyl**

***N*-[(10*R*,14*S*)-14-[1-(3-chlorophenyl)-5-oxopyrrolidine-3-amido]-10-methyl-9-oxo-8,16-diazatricyclo[13.3.1.0^{2,7}]nonadeca-1(19),2(7),3,5,15,17-hexaen-5-yl]carbamate, Trifluoroacetic acid salt (**11**, Diastereomer B).** A solution of **41**, 2TFA (0.015 g, 0.025 mmol), **43** (9.0 mg, 0.038 mmol), EDC (9.64 mg, 0.050 mmol), HOBT (7.70 mg, 0.050 mmol) and TEA (0.018 mL, 0.13 mmol) in DMF (1 mL) was warmed to 50 °C. After 2 h, the reaction was cooled to rt and then it was concentrated. Purification by reverse phase chromatography (solvent A: 10% ACN, 90% H₂O, 0.1% TFA and solvent B: 90% ACN, 10% H₂O, 0.1% TFA) gave **10** (first eluting diastereomer, diastereomer A, 6 mg, 34%) as a yellow solid. Diastereomer B (second eluting diastereomer) was obtained but contained impurities. Purification by reverse phase

1
2
3 chromatography (MeOH/water/TFA) gave **11** (diastereomer B, 3 mg, 17%) as a yellow solid.

4
5 Compound **10** (Diastereomer A): MS (ESI) m/z : 590.0 (M+H)⁺ and 592.0 (M+2+H)⁺. ¹H NMR
6
7 (500 MHz, CD₃OD) δ 9.63 (s, 1H, NH), 8.69 (d, $J=6.1$ Hz, 1H), 8.07 (d, $J=1.7$ Hz, 1H), 7.81
8
9 (dd, $J=5.9, 1.8$ Hz, 1H), 7.74 (t, $J=2.1$ Hz, 1H), 7.59 (d, $J=8.5$ Hz, 1H), 7.55 (d, $J=2.2$ Hz, 1H),
10
11 7.48 (dd, $J=8.5, 2.2$ Hz, 1H), 7.44 (br ddd, $J=8.3, 2.2, 0.8$ Hz, 1H), 7.32 (t, $J=8.0$ Hz, 1H), 7.16
12
13 (ddd, $J=8.0, 2.1, 1.0$ Hz, 1H), 5.08 (dd, $J=11.1, 5.9$ Hz, 1H), 4.10 – 4.05 (m, 1H), 3.95 (dd,
14
15 $J=9.8, 5.6$ Hz, 1H), 3.77 (s, 3H), 3.49 – 3.39 (m, 1H), 2.88 (dd, $J=17.3, 9.4$ Hz, 1H), 2.81 – 2.75
16
17 (m, 1H), 2.75 – 2.69 (m, 1H), 2.16 – 2.05 (m, 1H), 1.94 – 1.82 (m, 2H), 1.64 – 1.43 (m, 2H),
18
19 0.95 (d, $J=6.9$ Hz, 3H), 0.54 – 0.40 (m, 1H). Compound **11** (Diastereomer B): MS (ESI) m/z :
20
21 590.3 (M+H)⁺ and 592.3 (M+2+H)⁺. ¹H NMR (500 MHz, CD₃OD) δ 9.66 (s, 1H, NH), 8.71 (d,
22
23 $J=6.1$ Hz, 1H), 8.12 (s, 1H), 7.88 (br d, $J=5.8$ Hz, 1H), 7.76 (t, $J=2.1$ Hz, 1H), 7.63 (d, $J=8.5$ Hz,
24
25 1H), 7.57 (d, $J=1.7$ Hz, 1H), 7.49 (dd, $J=8.5, 2.2$ Hz, 1H), 7.46 (ddd, $J=8.3, 2.2, 0.8$ Hz, 1H),
26
27 7.34 (t, $J=8.3$ Hz, 1H), 7.17 (ddd, $J=8.0, 1.9, 0.8$ Hz, 1H), 5.08 (dd, $J=11.1, 5.9$ Hz, 1H), 4.16 -
28
29 4.08 (m, 1H), 4.01 - 3.95 (m, 1H), 3.77 (s, 3H), 3.48 - 3.40 (m, 1H), 2.89 - 2.80 (m, 1H), 2.79 -
30
31 2.70 (m, 2H), 2.17 - 2.06 (m, 1H), 1.92 - 1.81 (m, 2H), 1.64 - 1.43 (m, 2H), 0.95 (d, $J=6.9$ Hz,
32
33 3H), 0.54 - 0.41 (m, 1H).
34
35
36
37
38
39

40 **Methyl N-[(10R,14S)-14-[1-(3-chlorophenyl)pyrrolidine-3-amido]-10-methyl-9-oxo-**
41 **8,16-diazatricyclo[13.3.1.0^{2,7}]nonadeca-1(19),2(7),3,5,15,17-hexaen-5-yl]carbamate, Bis-**
42 **Trifluoroacetic acid salt, Diastereomeric mixture (12).** Using a procedure analogous to that
43
44 which was used to prepare **10** and **11**, compound **41**, 2TFA (0.020 g, 0.034 mmol) was coupled
45
46 with **45** (0.011 g, 0.050 mmol) to give **12** (0.012 g, 44%) as a mixture of diastereomers and as a
47
48 yellow solid. MS (ESI) m/z : 576.3 (M+H)⁺. ¹H NMR (500 MHz, CD₃OD) δ 8.77 - 8.69 (m, 1H),
49
50 8.18 (s, 1H), 7.97 - 7.88 (m, 1H), 7.65 - 7.59 (m, 1H), 7.57 (s, 1H), 7.53 - 7.46 (m, 1H), 7.13 -
51
52
53
54
55
56
57
58
59
60

1
2
3 7.05 (m, 1H), 6.61 - 6.54 (m, 1H), 6.53 - 6.48 (m, 1H), 6.48 - 6.40 (m, 1H), 5.08 (br dd, $J=10.6$,
4 5.9 Hz, 1H), 3.77 (s, 3H), 3.56 - 3.45 (m, 1H), 3.40 - 3.24 (m, 4H, overlaps with CD₃OD), 2.80 -
5 2.70 (m, 1H), 2.35 - 2.07 (m, 3H), 1.98 - 1.82 (m, 2H), 1.66 - 1.44 (m, 2H), 0.94 (br d, $J=6.9$ Hz,
6 3H), 0.53 - 0.39 (m, 1H).
7
8
9

10 Methyl

11
12 ***N*-[(10*R*,14*S*)-14-[1-(3-chlorophenyl)-1*H*-pyrazole-4-amido]-10-methyl-9-oxo-8,16-diazatric**
13 ***cyclo*[13.3.1.0^{2,7}]nonadeca-1(19),2(7),3,5,15,17-hexaen-5-yl]carbamate, Trifluoroacetic acid**
14 **salt (13).** Using a procedure analogous to that which was used to prepare **10** and **11**, compound
15 **41**, 2TFA (0.010 g, 0.017 mmol) was coupled with **48a** (5.60 mg, 0.025 mmol) to give **13** (4 mg,
16 34%) as a white solid. MS (ESI) m/z : 573.0 (M+H)⁺. ¹H NMR (500 MHz, CD₃OD) δ 8.81 (d,
17 $J=0.6$ Hz, 1H), 8.69 (d, $J=6.1$ Hz, 1H), 8.19 (s, 1H), 8.15 - 8.12 (m, 1H), 7.87 (t, $J=2.1$ Hz, 1H),
18 7.83 (dd, $J=6.1, 1.7$ Hz, 1H), 7.73 (ddd, $J=8.2, 2.1, 1.0$ Hz, 1H), 7.62 (d, $J=8.5$ Hz, 1H), 7.58 (d,
19 $J=1.9$ Hz, 1H), 7.53 - 7.48 (m, 2H), 7.39 (ddd, $J=8.0, 1.9, 0.8$ Hz, 1H), 5.25 (dd, $J=11.3, 6.1$ Hz,
20 1H), 3.77 (s, 3H), 2.81 - 2.71 (m, 1H), 2.25 - 2.13 (m, 1H), 2.04 - 1.88 (m, 2H), 1.67 - 1.46 (m,
21 2H), 0.97 (d, $J=6.9$ Hz, 3H), 0.59 - 0.42 (m, 1H).
22
23
24
25
26
27
28
29
30
31
32
33
34
35
36
37

38 Methyl

39
40 ***N*-[(10*R*,14*S*)-14-[1-(3-chloro-2-fluorophenyl)-1*H*-pyrazole-4-amido]-10-methyl-9-oxo-8,16-**
41 ***diazatricyclo*[13.3.1.0^{2,7}]nonadeca-1(19),2(7),3,5,15,17-hexaen-5-yl]carbamate,**
42 **Trifluoroacetic acid salt (14).** A clear, dull yellow solution of **48b** (9.08 mg, 0.038 mmol),
43 compound **41**, 2TFA (0.025 g, 0.042 mmol), EDC (0.012 g, 0.063 mmol), HOBT (9.63 mg,
44 0.063 mmol), and DIPEA (0.037 mL, 0.21 mmol) in DMF (0.42 mL) was stirred at rt overnight.
45 The reaction was diluted with MeOH and purification by reverse phase chromatography gave,
46 following concentration and lyophilization, **14** (0.0195 g, 64%) as a pale, yellow solid. MS
47
48
49
50
51
52
53
54
55
56
57
58
59
60

(ESI) m/z : 591.3 (M+H)⁺ and 593.2 (M+2+H)⁺. ¹H NMR (500 MHz, CD₃OD) δ 8.73 - 8.69 (m, 2H), 8.23 - 8.21 (m, 2H), 7.90 (dd, $J=6.1, 1.9$ Hz, 1H), 7.79 (ddd, $J=8.3, 6.9, 1.5$ Hz, 1H), 7.64 (d, $J=8.5$ Hz, 1H), 7.60 - 7.54 (m, 2H), 7.51 (dd, $J=8.5, 2.2$ Hz, 1H), 7.34 (td, $J=8.3, 1.7$ Hz, 1H), 5.27 (dd, $J=11.4, 5.9$ Hz, 1H), 3.78 (s, 3H), 2.82 - 2.73 (m, 1H), 2.25 - 2.14 (m, 1H), 2.05 - 1.90 (m, 2H), 1.67 - 1.48 (m, 2H), 0.97 (d, $J=6.9$ Hz, 3H), 0.57 - 0.44 (m, 1H). ¹⁹F NMR (471 MHz, CD₃OD) δ -77.29, -128.24.

Methyl

***N*-[(10*R*,14*S*)-14-[1-(2,3-dichlorophenyl)-1*H*-pyrazole-4-amido]-10-methyl-9-oxo-8,16-diazatricyclo[13.3.1.0^{2,7}]nonadeca-1(19),2(7),3,5,15,17-hexaen-5-yl]carbamate, Trifluoroacetic acid salt (15).** Using a procedure analogous to that which was used to prepare **10** and **11**, compound **41**, 2TFA (0.015 g, 0.025 mmol) was coupled with **48c** (6.46 mg, 0.025 mmol) to give **15** (0.010 g, 55%) as a yellow solid. MS (ESI) m/z : 607.3 (M+H)⁺ and 609.3 (M+2+H)⁺ and 611.3 (M+4+H)⁺. ¹H NMR (500 MHz, CD₃OD) δ 8.71 (d, $J=6.1$ Hz, 1H), 8.56 (s, 1H), 8.27 - 8.19 (m, 2H), 7.95 - 7.88 (m, 1H), 7.74 (dd, $J=8.0, 1.7$ Hz, 1H), 7.65 (br d, $J=8.5$ Hz, 1H), 7.62 - 7.58 (m, 1H), 7.57 - 7.46 (m, 3H), 5.27 (dd, $J=11.3, 6.1$ Hz, 1H), 3.78 (s, 3H), 2.81 - 2.73 (m, 1H), 2.26 - 2.16 (m, 1H), 2.06 - 1.87 (m, 2H), 1.69 - 1.48 (m, 2H), 0.97 (d, $J=7.2$ Hz, 3H), 0.59 - 0.45 (m, 1H).

Methyl

***N*-[(10*R*,14*S*)-14-[5-amino-1-(3-chlorophenyl)-1*H*-pyrazole-4-amido]-10-methyl-9-oxo-8,16-diazatricyclo[13.3.1.0^{2,7}]nonadeca-1(19),2(7),3,5,15,17-hexaen-5-yl]carbamate, Bis-trifluoroacetic acid salt (16).** Using a procedure analogous to that which was used to prepare **10** and **11**, compound **41**, 2TFA (0.010 g, 0.017 mmol) was coupled with **48d** to give **16** (6.0 mg, 43%) as a white solid. MS (ESI) m/z : 588.0 (M+H)⁺ and 590.0 (M+2+H)⁺. ¹H NMR (500 MHz,

1
2
3 CD₃OD) δ 9.69 (s, 1H, NH), 8.70 (d, $J=6.3$ Hz, 1H), 8.25 (d, $J=1.7$ Hz, 1H), 8.08 (s, 1H), 7.94
4
5 (dd, $J=6.2, 1.8$ Hz, 1H), 7.66 (d, $J=8.5$ Hz, 1H), 7.61 - 7.58 (m, 1H), 7.56 (t, $J=2.1$ Hz, 1H), 7.54
6
7 - 7.49 (m, 2H), 7.49 - 7.46 (m, 1H), 7.46 - 7.42 (m, 1H), 5.21 (dd, $J=11.3, 6.1$ Hz, 1H), 3.78 (s,
8
9 3H), 2.81 - 2.73 (m, 1H), 2.25 - 2.15 (m, 1H), 2.04 - 1.89 (m, 2H), 1.68 - 1.48 (m, 2H), 0.97 (d,
10
11 $J=6.9$ Hz, 3H), 0.57 - 0.44 (m, 1H).
12
13

14 Methyl

15
16
17 ***N*-[(10*R*,14*S*)-14-[5-amino-1-(3-chloro-2-fluorophenyl)-1H-pyrazole-4-amido]-10-methyl-9-**
18
19 **oxo-8,16-diazatricyclo[13.3.1.0^{2,7}]nonadeca-1(19),2(7),3,5,15,17-hexaen-5-yl]carbamate, *Bis*-**
20
21 **trifluoroacetic acid salt (17).** Using a procedure analogous to that which was used to prepare
22
23 **14**, compound **41**, 2HCl (0.020 g, 0.045 mmol) was coupled with **48e** (0.012 g, 0.045 mmol) to
24
25 give **17** (0.0192 g, 50%) as a pale yellow solid. MS (ESI) m/z : 606.4 (M+H)⁺ and 608.4
26
27 (M+2+H)⁺. ¹H NMR (500 MHz, CD₃OD) δ 8.70 (d, $J=6.3$ Hz, 1H), 8.23 (d, $J=1.4$ Hz, 1H), 8.11
28
29 (s, 1H), 7.92 (dd, $J=6.2, 1.8$ Hz, 1H), 7.67 - 7.62 (m, 2H), 7.58 (d, $J=1.9$ Hz, 1H), 7.52 (dd,
30
31 $J=8.5, 2.2$ Hz, 1H), 7.43 (ddd, $J=8.0, 6.5, 1.7$ Hz, 1H), 7.37 - 7.31 (m, 1H), 5.21 (dd, $J=11.3, 6.1$
32
33 Hz, 1H), 3.77 (s, 3H), 2.81 - 2.74 (m, 1H), 2.25 - 2.15 (m, 1H), 2.04 - 1.89 (m, 2H), 1.68 - 1.48
34
35 (m, 2H), 0.97 (d, $J=7.2$ Hz, 3H), 0.57 - 0.44 (m, 1H). ¹⁹F NMR (471 MHz, CD₃OD) δ -77.24, -
36
37 123.90.
38
39
40
41

42
43 **Methyl *N*-[(10*R*,14*S*)-14-[1-(3-chloro-2-fluorophenyl)-5-methyl-1H-pyrazole-4-**
44
45 **amido]-10-methyl-9-oxo-8,16-diazatricyclo[13.3.1.0^{2,7}]nonadeca-1(19),2(7),3,5,15,17-**
46
47 **hexaen-5-yl]carbamate, Trifluoroacetic acid salt and Hydrochloric acid salt (18).** To a vial
48
49 containing **50** (0.085 g, 0.34 mmol), compound **41**, 2TFA (0.200 g, 0.34 mmol), EDC (0.096 g,
50
51 0.50 mmol), and HOBT (0.077 g, 0.50 mmol) in DMF (4 mL) was added DIPEA (0.29 mL, 1.68
52
53 mmol). The reaction was stirred at rt overnight and then concentrated. Approximately half of
54
55
56
57
58
59
60

1
2
3 the crude residue was purified by reverse phase chromatography which gave, following
4
5 concentration and lyophilization, **18**, TFA salt (0.073 g, 30%) as an off-white solid. The other
6
7 half of the crude residue was purified by reverse phase chromatography and concentrated to give
8
9 a solid. The solid was dissolved in 1.25 M HCl in MeOH (2 mL) and the resulting solution was
10
11 concentrated. The solid was again dissolved in 1.25 M HCl in MeOH (2 mL) and the solution
12
13 was concentrated and then lyophilized which gave **18**, HCl salt (0.070 g, 32%) as a yellow solid.
14
15 Compound **18**, TFA: MS (ESI) m/z : 605.2 (M+H)⁺ and 607.1 (M+2+H)⁺. ¹H NMR (500 MHz,
16
17 CD₃OD) δ 8.69 (d, $J=6.1$ Hz, 1H), 8.30 (s, 1H), 8.14 - 8.09 (m, 1H), 7.81 (dd, $J=5.9$, 1.8 Hz,
18
19 1H), 7.71 (ddd, $J=8.1$, 6.7, 1.7 Hz, 1H), 7.62 (d, $J=8.5$ Hz, 1H), 7.57 (d, $J=1.9$ Hz, 1H), 7.50 (dd,
20
21 $J=8.5$, 2.2 Hz, 1H), 7.46 (ddd, $J=8.0$, 6.5, 1.7 Hz, 1H), 7.42 - 7.35 (m, 1H), 5.24 (dd, $J=11.4$, 5.9
22
23 Hz, 1H), 3.77 (s, 3H), 2.80 - 2.72 (m, 1H), 2.35 (d, $J=1.1$ Hz, 3H), 2.23 - 2.13 (m, 1H), 2.02 -
24
25 1.90 (m, 2H), 1.66 - 1.46 (m, 2H), 0.97 (d, $J=6.9$ Hz, 3H), 0.57 - 0.43 (m, 1H). ¹⁹F NMR (471
26
27 MHz, CD₃OD) δ -77.15, -125.44. Compound **18**, HCl: MS (ESI) m/z : 605.2 (M+H)⁺ and 607.1
28
29 (M+2+H)⁺. ¹H NMR (500 MHz, CD₃OD) δ 8.74 (d, $J=6.3$ Hz, 1H), 8.41 (s, 1H), 8.32 (d, $J=1.7$
30
31 Hz, 1H), 7.99 (dd, $J=6.2$, 1.8 Hz, 1H), 7.71 (br ddd, $J=8.3$, 6.7, 1.5 Hz, 1H), 7.65 (d, $J=8.5$ Hz,
32
33 1H), 7.59 - 7.52 (m, 2H), 7.46 (ddd, $J=8.0$, 6.5, 1.7 Hz, 1H), 7.41 - 7.36 (m, 1H), 5.30 (dd,
34
35 $J=11.6$, 6.1 Hz, 1H), 3.77 (s, 3H), 2.86 - 2.77 (m, 1H), 2.37 - 2.33 (m, 3H), 2.29 - 2.19 (m, 1H),
36
37 2.14 - 2.04 (m, 1H), 2.02 - 1.91 (m, 1H), 1.71 - 1.51 (m, 2H), 0.97 (d, $J=7.2$ Hz, 3H), 0.58 - 0.44
38
39 (m, 1H). ¹⁹F NMR (471 MHz, CD₃OD) δ -125.44.

40
41
42 **Methyl N-[(10R,14S)-14-[1-(3-chloro-2-fluorophenyl)-5-methyl-1H-imidazole-4-**
43
44 **amido]-10-methyl-9-oxo-8,16-diazatricyclo[13.3.1.0^{2,7}]nonadeca-1(19),2(7),3,5,15,17-**
45
46 **hexaen-5-yl]carbamate, Bis-trifluoroacetic acid salt and Bis-hydrochloric acid salt (19).** A
47
48 cloudy, gray mixture of **52** (0.620 g, 2.13 mmol), compound **41**, 2TFA (1.27 g, 2.13 mmol),
49
50
51
52
53
54
55
56
57
58
59
60

1
2
3 EDC (0.612 g, 3.19 mmol), HOBT (0.489 g, 3.19 mmol), and DIPEA (1.86 mL, 10.6 mmol) in
4 DMF (21.3 mL) was stirred at rt. After 18 h, the reaction was cooled to 0 °C and water (42 mL)
5
6 was added slowly to give a suspension. The mixture was stirred for 1h. The reaction was
7
8 extracted with EtOAc (3x). The organic layers were combined, washed with sat. NaHCO₃,
9
10 brine, dried over Na₂SO₄, filtered and concentrated to give an off-white solid. Purification by
11
12 normal phase chromatography (0-10% MeOH/DCM) gave **19** (1.04 g, 77%) as the free base and
13
14 as a white solid. A portion of the free base was purified by reverse phase chromatography
15
16 (MeOH:H₂O:TFA) which gave, after concentration and lyophilization, **19**, 2TFA as a fluffy
17
18 yellow solid. Another portion of the free base was purified by reverse phase chromatography
19
20 (gradient elution 10-100% B; solvent A: 10:90:0.05 ACN:H₂O:HCl and solvent B: 90:10:0.1
21
22 ACN:H₂O:HCl) which gave, after concentration and lyophilization, **19**, 2HCl as a fluffy, yellow
23
24 solid. Compound **19**, free base: MS (ESI) *m/z*: 605.2 (M+H)⁺ and 607.1 (M+2+H)⁺. ¹H NMR
25
26 (400 MHz, CD₃OD) δ 8.61 (d, *J*=5.1 Hz, 1H), 7.74 (br s, 1H), 7.71 (ddd, *J*=8.1, 6.7, 1.7 Hz, 1H),
27
28 7.61 (s, 1H), 7.50 (d, *J*=8.6 Hz, 1H), 7.49 - 7.42 (m, 3H), 7.41 - 7.35 (m, 2H), 5.22 (dd, *J*=10.7,
29
30 5.6 Hz, 1H), 3.76 (s, 3H), 2.75 - 2.66 (m, 1H), 2.36 (d, *J*=0.7 Hz, 3H), 2.14 - 2.01 (m, 1H), 1.99 -
31
32 1.87 (m, 1H), 1.87 - 1.74 (m, 1H), 1.58 - 1.32 (m, 2H), 0.94 (d, *J*=7.0 Hz, 3H), 0.51 - 0.34 (m,
33
34 1H). ¹⁹F NMR (471 MHz, CD₃OD) δ -125.7. Anal. Calc'd for C₃₁H₃₀ClF₆O₄ · 0.16 H₂O: C,
35
36 61.25; H, 5.03; N, 13.82; Cl, 5.83. Found: C, 61.58; H, 5.05; N, 13.80; Cl, 5.90. Compound **19**,
37
38 2TFA: ¹H NMR (400 MHz, CD₃OD) δ 9.65 (s, 1H, NH), 8.72 (d, *J*=6.2 Hz, 1H), 8.17 (d, *J*=1.3
39
40 Hz, 1H), 7.86 (dd, *J*=6.2, 1.8 Hz, 1H), 7.81 (s, 1H), 7.72 (ddd, *J*=8.1, 6.7, 1.8 Hz, 1H), 7.63 (d,
41
42 *J*=8.6 Hz, 1H), 7.58 (d, *J*=2.0 Hz, 1H), 7.51 (dd, *J*=8.6, 2.2 Hz, 1H), 7.47 - 7.37 (m, 2H), 5.29
43
44 (dd, *J*=11.1, 6.1 Hz, 1H), 3.77 (s, 3H), 2.83 - 2.71 (m, 1H), 2.32 (s, 3H), 2.27 - 2.13 (m, 1H),
45
46 2.05 - 1.87 (m, 2H), 1.71 - 1.45 (m, 2H), 0.96 (d, *J*=6.8 Hz, 3H), 0.57 - 0.40 (m, 1H). ¹⁹F NMR
47
48
49
50
51
52
53
54
55
56
57
58
59
60

(376 MHz, CD₃OD) δ -77.2, -125.8. ¹³C NMR (126 MHz, CD₃OD) δ 176.1, 165.8, 158.6, 156.5, 156.1, 154.6 (d, $J=252$ Hz), 144.4 (overlap of two carbons based in HMQC and HMBC analysis), 138.5, 137.5, 136.2, 133.6, 131.7, 131.5, 129.1, 128.0, 127.0 (d, $J=5.8$ Hz), 125.9, 125.7 (d, $J=11.6$ Hz), 125.3, 123.7 (d, $J=16.2$ Hz), 118.2, 117.5, 53.1, 52.9, 40.4, 32.3, 30.5, 20.3, 14.2, 9.8. Compound **19**, 2HCl: ¹H NMR (400 MHz, CD₃OD) δ 8.76 (d, $J=6.2$ Hz, 1H), 8.34 (d, $J=1.5$ Hz, 1H), 8.07 (s, 1H), 8.01 (dd, $J=6.2, 1.8$ Hz, 1H), 7.75 (ddd, $J=8.1, 6.7, 1.7$ Hz, 1H), 7.68 (d, $J=8.6$ Hz, 1H), 7.60 (d, $J=2.0$ Hz, 1H), 7.53 (dd, $J=8.5, 2.1$ Hz, 1H), 7.51 - 7.46 (m, 1H), 7.42 (dt, $J=8.1, 1.3$ Hz, 1H), 5.33 (dd, $J=11.2, 6.2$ Hz, 1H), 3.78 (s, 3H), 2.89 - 2.73 (m, 1H), 2.34 (s, 3H), 2.32 - 2.20 (m, 1H), 2.11 - 1.89 (m, 2H), 1.75 - 1.50 (m, 2H), 0.97 (d, $J=7.0$ Hz, 3H), 0.61 - 0.42 (m, 1H). ¹⁹F NMR (376 MHz, CD₃OD) δ -125.8.

Methyl N-[(10*R*,14*S*)-14-[1-(3-chloro-2-fluorophenyl)-5-methyl-1*H*-1,2,3-triazole-4-amido]-10-methyl-9-oxo-8,16-diazatricyclo[13.3.1.0^{2,7}]nonadeca-1(19),2(7),3,5,15,17-hexaen-5-yl]carbamate, Trifluoroacetic acid salt and Hydrochloric acid salt (20**). A clear, yellow solution of **54** (0.290 g, 1.13 mmol), compound **41**, 2HCl (0.500 g, 1.13 mmol), EDC (0.326 g, 1.70 mmol), HOBT (0.260 g, 1.70 mmol), and DIPEA (0.980 mL, 5.66 mmol) in DMF (11.3 mL) was stirred at rt. After 24 h, H₂O (33 mL) was added to give a suspension. The mixture was stirred for 15 min. The solid was collected by filtration, rinsed with water, air-dried, and dried under vacuum to give an off-white solid weighing 0.650 g. The off-white solid was suspended in MeOH (30 mL), sonicated and then warmed to a gentle reflux. The solid was collected by filtration, rinsed with MeOH, air-dried, and dried under vacuum to give **20** (0.360 g, 52%) as the free base and as a white solid. Compound **20**, free base (0.060 g) was dissolved in 1:1 DMF/MeOH (2 mL) with a few drops of TFA. Purification by reverse phase chromatography gave, after concentration and lyophilization, **20**, TFA salt (0.0548 g) as a white**

1
2
3 solid. Compound **20**, free base (290 mg) was dissolved in ACN (9 mL) and 1.0 M HCl (0.65
4 mL). Purification by reverse phase chromatography (gradient elution 10-100% B; solvent A:
5
6 10:90:0.05 ACN:H₂O:HCl and solvent B: 90:10:0.1 ACN:H₂O:HCl) gave, following
7
8 concentration and lyophilization, **20**, HCl (0.121 g) as a yellow solid. Compound **20**, free base:
9
10 MS (ESI) *m/z*: 606.4 (M+H)⁺ and 608.4 (M+H)⁺. ¹H NMR (400 MHz, DMSO-d₆) δ 9.90 (s, 1H,
11
12 NH), 9.72 (s, 1H, NH), 8.63 (d, *J*=5.1 Hz, 1H), 8.55 (d, *J*=7.5 Hz, 1H, NH), 7.94 (ddd, *J*=8.3,
13
14 6.9, 1.5 Hz, 1H), 7.74 (td, *J*=7.4, 1.5 Hz, 1H), 7.59 (s, 1H), 7.56 - 7.45 (m, 3H), 7.37 (d, *J*=1.8
15
16 Hz, 1H), 7.33 (dd, *J*=5.3, 1.5 Hz, 1H), 5.24 - 5.14 (m, 1H), 3.70 (s, 3H), 2.72 - 2.58 (m, 1H),
17
18 2.44 (s, 3H), 2.07 - 1.92 (m, 1H), 1.92 - 1.79 (m, 1H), 1.79 - 1.65 (m, 1H), 1.48 - 1.31 (m, 1H),
19
20 1.31 - 1.16 (m, 1H), 0.84 (d, *J*=6.8 Hz, 3H), 0.41 - 0.18 (m, 1H). ¹³C NMR (126 MHz, DMSO) δ
21
22 172.4, 159.4, 157.4, 153.9, 151.8 (d, *J* = 253.1 Hz), 150.2, 146.7, 140.2, 138.4, 137.6, 136.1,
23
24 133.2, 129.7, 129.5, 127.9, 126.1 (d, *J* = 3.5 Hz), 124.0 (d, *J* = 12.6 Hz), 121.4, 121.2 (d, *J* =
25
26 15.0 Hz), 121.2, 117.2, 116.4, 51.9, 51.8, 38.1, 33.0, 29.6, 19.2, 14.5, 8.5. ¹⁹F NMR (376 MHz,
27
28 DMSO-d₆) δ -124.10. Compound **20**, TFA salt: MS (ESI) *m/z*: 606.3 (M+H)⁺ and 608.2 (M+H)⁺.
29
30 ¹H NMR (500 MHz, DMSO-d₆) δ 9.93 (s, 1H, NH), 9.77 (s, 1H, NH), 8.67 (d, *J*=5.2 Hz, 1H),
31
32 8.62 (br d, *J*=7.2 Hz, 1H, NH), 7.94 (ddd, *J*=8.3, 6.8, 1.7 Hz, 1H), 7.74 (ddd, *J*=8.1, 6.7, 1.7 Hz,
33
34 1H), 7.71 - 7.65 (m, 1H), 7.55 - 7.51 (m, 2H), 7.49 (td, *J*=9.1, 1.8 Hz, 1H), 7.45 - 7.40 (m, 1H),
35
36 7.38 (d, *J*=1.9 Hz, 1H), 5.25 - 5.18 (m, 1H), 3.70 (s, 3H), 2.71 - 2.60 (m, 1H), 2.43 (s, 3H), 2.07 -
37
38 1.93 (m, 1H), 1.92 - 1.81 (m, 1H), 1.81 - 1.69 (m, 1H), 1.45 - 1.33 (m, 1H), 1.31 - 1.20 (m, 1H),
39
40 0.83 (d, *J*=7.2 Hz, 3H), 0.37 - 0.20 (m, 1H). ¹⁹F NMR (471 MHz, DMSO-d₆) δ -73.99, -124.11.
41
42
43
44
45
46
47
48
49 Compound **20**, HCl salt: MS (ESI) *m/z*: 606.2 (M+H)⁺ and 608.2 (M+H)⁺. ¹H NMR (500 MHz,
50
51 CD₃OD) δ 9.70 (s, 1H, NH), 8.75 (d, *J*=6.1 Hz, 1H), 8.29 (d, *J*=1.4 Hz, 1H), 7.95 (dd, *J*=6.2, 1.8
52
53 Hz, 1H), 7.82 (ddd, *J*=8.3, 6.8, 1.7 Hz, 1H), 7.66 (d, *J*=8.5 Hz, 1H), 7.60 (d, *J*=1.9 Hz, 1H), 7.56
54
55
56
57
58
59
60

(ddd, $J=8.1, 6.5, 1.7$ Hz, 1H), 7.53 (dd, $J=8.5, 2.2$ Hz, 1H), 7.49 - 7.43 (m, 1H), 5.37 (dd, $J=11.4, 6.2$ Hz, 1H), 3.78 (s, 3H), 2.83 - 2.76 (m, 1H), 2.43 (d, $J=0.8$ Hz, 3H), 2.31 - 2.22 (m, 1H), 2.09 - 1.92 (m, 2H), 1.72 - 1.51 (m, 2H), 0.97 (d, $J=7.2$ Hz, 3H), 0.58 - 0.42 (m, 1H). ^{19}F NMR (471 MHz, CD_3OD) δ -125.29.

Methyl

***N*-[(10*R*,14*S*)-14-[3-(3-chloro-2-fluorophenyl)-4-methyl-1,2-oxazole-5-amido]-10-methyl-9-oxo-8,16-diazatricyclo[13.3.1.0^{2,7}]nonadeca-1(19),2(7),3,5,15,17-hexaen-5-yl]carbamate,**

Trifluoroacetic acid salt (21). Using a procedure analogous to that which was used to prepare **14**, compound **41**, 2TFA (0.023 g, 0.039 mmol) was coupled with **57** (0.0099 g, 0.039 mmol) to give **21** (8 mg, 28%) as a white solid. MS (ESI) m/z : 606.2 (M+H)⁺. ^1H NMR (500 MHz, CD_3OD) δ 8.71 (d, $J=6.1$ Hz, 1H), 8.15 (d, $J=1.4$ Hz, 1H), 7.84 (dd, $J=5.9, 1.8$ Hz, 1H), 7.72 - 7.67 (m, 1H), 7.64 (d, $J=8.5$ Hz, 1H), 7.58 (d, $J=2.2$ Hz, 1H), 7.51 (dd, $J=8.5, 2.2$ Hz, 1H), 7.49 - 7.45 (m, 1H), 7.38 - 7.33 (m, 1H), 5.31 (dd, $J=11.3, 6.1$ Hz, 1H), 3.78 (s, 3H), 2.81 - 2.71 (m, 1H), 2.27 - 2.15 (m, 4H), 2.06 - 1.87 (m, 2H), 1.67 - 1.45 (m, 2H), 0.97 (d, $J=6.9$ Hz, 3H), 0.61 - 0.43 (m, 1H). ^{19}F NMR (471 MHz, CD_3OD) δ -77.39, -117.93.

Methyl

***N*-[(10*R*,14*S*)-14-[5-(3-chloro-2-fluorophenyl)-4-methyl-1,2-oxazole-3-amido]-10-methyl-9-oxo-8,16-diazatricyclo[13.3.1.0^{2,7}]nonadeca-1(19),2(7),3,5,15,17-hexaen-5-yl]carbamate,**

Trifluoroacetic acid salt (22). Using a procedure analogous to that which was used to prepare **14**, compound **41**, 2TFA (0.019 g, 0.032 mmol) was coupled with **60** (0.0081 g, 0.032 mmol) at 55°C to give **22** (8.2 mg, 34%) as a white solid. MS (ESI) m/z : 606.1 (M+H)⁺. ^1H NMR (500 MHz, CD_3OD) δ 8.75 (d, $J=6.3$ Hz, 1H), 8.25 (d, $J=1.4$ Hz, 1H), 7.93 (dd, $J=6.1, 1.9$ Hz, 1H), 7.72 - 7.68 (m, 1H), 7.66 (d, $J=8.5$ Hz, 1H), 7.60 (d, $J=1.9$ Hz, 1H), 7.57 - 7.50 (m, 2H), 7.36 (td,

1
2
3 $J=8.0, 0.8$ Hz, 1H), 5.35 (dd, $J=11.6, 6.1$ Hz, 1H), 3.78 (s, 3H), 2.82 - 2.71 (m, 1H), 2.28 - 2.18
4 (m, 1H), 2.17 (d, $J=2.2$ Hz, 3H), 2.08 - 1.88 (m, 2H), 1.70 - 1.46 (m, 2H), 0.97 (d, $J=6.9$ Hz,
5
6 3H), 0.58 - 0.43 (m, 1H). ^{19}F NMR (471 MHz, CD_3OD) δ -77.47, -116.35.
7
8
9

10 **(S)-N-[(1E)-(4-Chloropyridin-2-yl)methylidene]-2-methylpropane-2-sulfinamide**

11
12 **(25)**. To a solution of **24**⁵¹ (10 g, 70.6 mmol) in DCM (200 mL) was added (S)-2-methylpropane-
13 2-sulfinamide (9.42 g, 78 mmol) followed by Cs_2CO_3 (34.5 g, 106 mmol). The reaction mixture
14 was stirred at rt overnight. Then the reaction mixture was diluted with H_2O (100 mL) and the
15 layers were separated. The aqueous layer was extracted with EtOAc (100 mL). The organic
16 layers were combined, dried over Na_2SO_4 , filtered, and concentrated. Purification by normal
17 phase chromatography (0-20% EtOAc/petroleum ether) gave **25** (16.3 g, 94%) as a yellow liquid
18 which can solidify to give a yellow solid. MS (ESI) m/z : 245.0 (M+H)⁺. ^1H NMR (500 MHz,
19 CDCl_3) δ 8.68 (s, 1H), 8.65 (d, $J=5.5$ Hz, 1H), 8.03 (d, $J=2.2$ Hz, 1H), 7.42 (dd, $J=5.2, 1.9$ Hz,
20 1H), 1.30 (s, 9H). ^{13}C NMR (126 MHz, CDCl_3) δ 162.7, 153.8, 150.9, 145.0, 125.9, 122.9, 58.3,
21 22.6. $[\alpha]_{\text{D}} = +69.2$ (c = 1.24, CHCl_3).
22
23
24
25
26
27
28
29
30
31
32
33
34
35

36 **tert-Butyl N-[(1S)-1-(4-chloropyridin-2-yl)but-3-en-1-yl]carbamate (27)**. To a cooled
37 (0-5 °C) mixture of InCl_3 (13.56 g, 61.3 mmol) in THF (170 mL) was added dropwise over 30
38 min. allylmagnesium bromide (62 mL, 61.3 mmol, 1 M in Et_2O). The reaction was allowed to
39 warm to rt. After 1 h at rt, a solution of **25** (10 g, 40.9 mmol) in EtOH (170 mL) was added.
40 After 2-3 h, the reaction was concentrated under vacuum at 50-55 °C. The crude material was
41 partitioned between EtOAc (200 mL) and H_2O (50 mL) and the layers were separated. The
42 aqueous layer was extracted with EtOAc (2x50 mL). The organic layers were combined and
43 washed with brine (100 mL), dried over Na_2SO_4 , filtered and concentrated to give **26** (13.5 g,
44 106%) as a yellow oil. This material was used in the next step without further purification. MS
45
46
47
48
49
50
51
52
53
54
55
56
57
58
59
60

(ESI) m/z : 287.1 (M+H)⁺. ¹H NMR (500 MHz, CD₃OD) δ 8.45 (d, J =5.5 Hz, 1H), 7.60 (d, J =1.6 Hz, 1H), 7.36 (dd, J =5.5, 2.2 Hz, 1H), 5.82 - 5.72 (m, 1H), 5.09 - 5.01 (m, 2H), 4.46 (t, J =7.1 Hz, 1H), 2.62 - 2.57 (m, 2H), 1.24 (s, 9H).

To a solution of **26** (7.04 g, 24.5 mmol) in MeOH (75 mL) was added 4 M HCl in dioxane (30.7 mL, 123 mmol). The reaction was stirred at rt for 1 h and then the reaction was concentrated to give a pink white solid. The solid was suspended in MeCN (75 mL) and then Boc₂O (10.7 g, 49.1 mmol) and TEA (34.2 mL, 245 mmol) were added. The reaction mixture was stirred at rt for 21 h. Then, the reaction mixture was diluted with EtOAc, washed with brine, dried over MgSO₄, filtered and concentrated to give a dark orange brown oil. Purification by normal phase chromatography (0-40% EtOAc/Hex) gave **27** (7.0 g, 100%) as a clear, yellow oil which forms a white solid upon sitting in the freezer. The %ee was improved to >99%ee by preparative supercritical fluid chromatography (SFC) using the following conditions: Regis Whelk-01(R,R) [250 mm x 30 mm, 5 μ m], 5% IPA in CO₂, 70 mL/min, 100 Bar, 35 °C, and UV detection at 210 nm. The analytical SFC conditions were the following: Regis Whelk-01(R,R) [250 mm X 4.6 mm, 5 μ m], 5% IPA in CO₂, 2.2 mL/min, 100 Bar, 35 °C, and UV detection at 220 nm. Peak 1 was the desired enantiomer at 5.4 min. Peak 2 was the undesired enantiomer at 6.9 min. MS (ESI) m/z : 227.3 (M-C₄H₈+H)⁺ and 305.4 (M+Na)⁺. ¹H NMR (500 MHz, CDCl₃) δ 8.45 (d, J =5.2 Hz, 1H), 7.24 (d, J =1.7 Hz, 1H), 7.18 (dd, J =5.4, 2.1 Hz, 1H), 5.70 - 5.61 (m, 1H), 5.51 - 5.40 (m, 1H), 5.12 - 5.00 (m, 2H), 4.84 - 4.74 (m, 1H), 2.64 - 2.51 (m, 2H), 1.43 (br s, 9H). ¹³C NMR (126 MHz, CDCl₃) δ 162.1, 155.2, 150.1, 144.3, 133.3, 122.5, 121.9, 118.4, 79.5, 54.8, 40.4, 28.3. $[\alpha]_D = -41.5$ (c = 1.33, CHCl₃).

tert-Butyl N-[(1S)-1-[4-(2-amino-4-nitrophenyl)pyridin-2-yl]but-3-en-1-yl]carbamate (29). To a RBF was added **27** (3.33 g, 11.8 mmol), **28** (5.89 g, 23.6 mmol), PdCl₂(dppf)-CH₂Cl₂

1
2
3 adduct (0.962 g, 1.18 mmol), and K_3PO_4 (5.00 g, 23.6 mmol). The RBF was equipped with a
4
5 reflux condenser then the apparatus was purged with argon for several minutes. Next, degassed
6
7 DMSO (59 mL) was added followed by degassed H_2O (1.06 mL, 58.9 mmol). The resulting
8
9 bright orange suspension was warmed to 90 °C. After 6 h, the dark black reaction mixture was
10
11 cooled to rt. The reaction was filtered to remove the solid and the solid was rinsed with EtOAc.
12
13 The filtrate was partitioned between EtOAc, water, and brine (to break up the emulsion) and the
14
15 layers were separated. The aqueous layer was extracted with EtOAc (1x). The organic layers
16
17 were combined, washed with brine, dried over Na_2SO_4 , filtered and concentrated to give a thick,
18
19 black oil. Purification by normal phase chromatography (gradient elution 0-40% EtOAc/Hex)
20
21 gave 2.90 g of **29** as an orange foam and 0.97 g of impure material. The impure material was
22
23 repurified as described above to give 0.66 g of **29** as an orange foam. The two batches were
24
25 combined to give **29** (3.56 g, 78%) as an orange foam. MS (ESI) m/z : 385.1 (M+H)⁺. ¹H NMR
26
27 (500 MHz, CD_3OD) δ 8.59 (d, $J=4.9$ Hz, 1H), 7.66 (d, $J=2.7$ Hz, 1H), 7.53 (dd, $J=8.2, 2.2$ Hz,
28
29 1H), 7.50 (s, 1H), 7.40 (br d, $J=4.4$ Hz, 1H), 7.26 (d, $J=8.2$ Hz, 1H), 5.89 - 5.76 (m, 1H), 5.10 (br
30
31 d, $J=17.6$ Hz, 1H), 5.06 (br d, $J=10.4$ Hz, 1H), 4.80 - 4.70 (m, 1H), 2.71 - 2.56 (m, 1H), 2.56 -
32
33 2.40 (m, 1H), 1.42 (s, 9H). ¹³C NMR (126 MHz, CD_3OD) δ 163.8, 158.0, 150.8, 150.5, 148.9,
34
35 147.7, 135.7, 132.1, 130.5, 123.5, 122.2, 118.4, 112.7, 110.9, 80.7, 57.3, 41.0, 28.9. $[\alpha]_D = -49.0$
36
37 (c = 1.19, MeOH).
38
39

40 41 42 ***tert*-Butyl**

43
44
45 ***N*-[(1*S*)-1-{4-[2-(*but*-3-enamido)-4-nitrophenyl]pyridin-2-yl}but-3-en-1-yl]carbamate (**30**).**

46
47
48 To a cooled (-5 °C) clear, yellow solution of **29** (0.200 g, 0.52 mmol) and *but*-3-enoic acid (0.081
49
50 mL, 1.04 mmol) in EtOAc (5.20 mL) was added DIPEA (0.27 mL, 1.56 mmol) and T₃P (50 wt%
51
52 in EtOAc, 0.61 mL, 1.04 mmol). Following the addition, the reaction was allowed to warm to rt.
53
54
55
56
57
58
59
60

1
2
3 After 2.5 h, the reaction was diluted with EtOAc and washed with sat. NaHCO₃. The aqueous
4 layer was extracted with EtOAc (1x). The organic layers were combined, washed with brine,
5
6 dried over Na₂SO₄, filtered and concentrated to give a yellow oil. Purification by normal phase
7
8 chromatography (gradient elution 0-50% EtOAc/Hex) gave **30** (0.207 g, 88 %) as a pale, yellow
9
10 foam. MS (ESI) *m/z*: 453.3 (M+H)⁺. ¹H NMR (500 MHz, CD₃OD) δ 8.60 (d, *J*=5.2 Hz, 1H),
11
12 8.57 (br s, 1H), 8.22 - 8.15 (m, 1H), 7.60 (br d, *J*=8.5 Hz, 1H), 7.43 (s, 1H), 7.34 (br d, *J*=4.4 Hz,
13
14 1H), 5.95 - 5.85 (m, 1H), 5.85 - 5.75 (m, 1H), 5.19 - 5.13 (m, 2H), 5.10 (br d, *J*=17.1 Hz, 1H),
15
16 5.06 (br d, *J*=10.2 Hz, 1H), 4.81 - 4.75 (m, 1H), 3.09 (br d, *J*=6.6 Hz, 2H), 2.67 - 2.58 (m, 1H),
17
18 2.55 - 2.46 (m, 1H), 1.42 (s, 9H). ¹³C NMR (126 MHz, CD₃OD) δ 172.6, 163.7, 157.8, 150.5,
19
20 149.5, 147.9, 140.9, 137.1, 135.6, 132.4, 132.2, 123.6, 122.5, 122.0, 121.9, 119.7, 118.5, 80.6,
21
22 57.3, 42.3, 41.2, 28.9. [α]_D = -38.86 (c = 1.02, MeOH).
23
24
25
26
27
28

29 Methyl

30
31 ***N*-[3-(but-3-enamido)-4-{2-[(1*S*)-1-{{*tert*-butoxy}carbonyl}amino}but-3-en-1-yl]pyridin-4-yl**
32
33 **}phenyl]carbamate (31)**. To a clear, yellow solution of **30** (0.100 g, 0.22 mmol) in MeOH (4.4
34 mL) was added zinc dust (0.145 g, 2.21 mmol) and NH₄Cl (0.118 g, 2.21 mmol). The gray
35 suspension was stirred vigorously at rt. After 2.5 h, the reaction was filtered through a 0.45
36 micron nylon filter, eluting with MeOH. The filtrate was concentrated to give a clear, pale
37 yellow residue. The residue was partitioned between EtOAc and 0.25 M HCl (7 mL) and the
38 layers were separated. The organic layer was extracted with 0.25 M HCl (2 x 7 mL). The acid
39 layers were combined, neutralized with 1.5 M K₂HPO₄ and then extracted with EtOAc (3x). The
40 organic layers were combined, washed with brine, dried over Na₂SO₄, filtered and concentrated
41 to give *tert*-butyl
42
43
44
45
46
47
48
49
50
51
52

53
54 ***N*-[(1*S*)-1-{4-[4-amino-2-(but-3-enamido)phenyl]pyridin-2-yl}but-3-en-1-yl]carbamate (0.0927**
55
56
57
58
59
60

g, 99 %) as a pale, yellow foam. MS (ESI) m/z : 423.3 (M+H)⁺. The material was used in the next step without further purification.

To a cooled (-5 °C) clear, pale yellow solution of *tert*-butyl *N*-[(1*S*)-1-{4-[4-amino-2-(but-3-enamido)phenyl]pyridin-2-yl}but-3-en-1-yl]carbamate (0.0927 g, 0.22 mmol) in DCM (2.2 mL) was added pyridine (0.018 mL, 0.22 mmol) and methyl chloroformate (0.017 mL, 0.22 mmol). The resulting bright yellow solution was stirred at -5 °C. After 30 min, a white suspension formed and more DCM (1 mL) was added to facilitate mixing. After 1 h, the reaction was stopped, diluted with EtOAc, and washed with sat. NaHCO₃. The aqueous layer was extracted with EtOAc (2x). The organic layers were combined, washed with brine, dried over Na₂SO₄, filtered and concentrated to give a white foam. Purification by normal phase chromatography (0-70% EtOAc/Hex) gave **31** (0.0902 g, 86% over two steps) as a clear, colorless residue. MS (ESI) m/z : 481.4 (M+H)⁺. ¹H NMR (500 MHz, CD₃OD) δ 8.48 (d, J =4.9 Hz, 1H), 7.66 (s, 1H), 7.48 (dd, J =8.2, 2.2 Hz, 1H), 7.37 (s, 1H), 7.31 (d, J =8.2 Hz, 1H), 7.27 (br d, J =4.4 Hz, 1H), 5.94 - 5.74 (m, 2H), 5.18 - 5.02 (m, 4H), 4.79 - 4.72 (m, 1H), 3.75 (s, 3H), 3.03 (br d, J =7.1 Hz, 2H), 2.65 - 2.56 (m, 1H), 2.52 - 2.43 (m, 1H), 1.46 - 1.31 (m, 9H, rotamers of Boc group). ¹³C NMR (126 MHz, CD₃OD) δ 172.7, 163.0, 157.8, 156.3, 149.9, 141.7, 136.0, 135.7, 132.5, 131.7, 130.4, 123.9, 122.7, 119.3, 118.4, 118.0, 80.5, 57.2, 52.8, 42.3, 41.3, 28.9.

Note: two carbons overlap.

Methyl

N-(3-amino-4-{2-[(1*S*)-1-[(*tert*-butoxy)carbonyl]amino]but-3-en-1-yl}pyridin-4-yl}phenyl)carbamate (**32**). To a clear, orange solution of **29** (2.9 g, 7.54 mmol) in MeOH (75 mL) was added sequentially zinc dust (4.93 g, 75 mmol) and NH₄Cl (4.0 g, 75 mmol). The resulting suspension was stirred vigorously for 4 h. The reaction was stopped and filtered through a 0.45

micron, glass membrane filter, eluting with MeOH, to give a clear, yellow filtrate.

Concentration of the filtrate gave a yellow-black residue. The residue was partitioned between EtOAc and 0.25 M HCl (50 mL) and the layers were separated. The organic layer was extracted with 0.25 M HCl (50 mL). The combined acid layers were neutralized with 1.5 M K₂HPO₄ and then extracted with EtOAc (3x). The organic layers were combined, washed with brine, dried over Na₂SO₄, filtered and concentrated to give *tert*-butyl *N*-[(1*S*)-1-[4-(2,4-diaminophenyl)pyridin-2-yl]but-3-en-1-yl]carbamate (2.63 g, 98%) as a brown foam. MS (ESI) *m/z*: 355.1 (M+H)⁺. ¹H NMR (500 MHz, CD₃OD) δ 8.42 (d, *J*=5.2 Hz, 1H), 7.45 (d, *J*=1.4 Hz, 1H), 7.34 (br d, *J*=4.4 Hz, 1H), 6.93 - 6.89 (m, 1H), 6.23 - 6.19 (m, 2H), 5.86 - 5.75 (m, 1H), 5.09 (dd, *J*=17.1, 1.4 Hz, 1H), 5.05 (br d, *J*=10.2 Hz, 1H), 4.75 - 4.68 (m, 1H), 2.66 - 2.56 (m, 1H), 2.51 - 2.42 (m, 1H), 1.42 (s, 9H).

To a cooled (-78 °C) clear, brown solution of *tert*-butyl *N*-[(1*S*)-1-[4-(2,4-diaminophenyl)pyridin-2-yl]but-3-en-1-yl]carbamate (2.63 g, 7.42 mmol) and pyridine (0.60 mL, 7.42 mmol) in DCM (74 mL) was added dropwise over 30 min. methyl chloroformate (0.52 mL, 6.68 mmol). The reaction was stirred at -78 °C. After 1.5 h, the reaction was quenched with sat. NH₄Cl and the reaction was allowed to warm to rt. The reaction was diluted with DCM and water and then the layers were separated. The aqueous layer was extracted with DCM. The organic layers were combined, washed with saturated NaHCO₃, brine, dried over Na₂SO₄, filtered and concentrated to give a brown foam. The brown foam was dissolved in DCM (~10 mL) and then hexane (~300 mL) was added to give a brown suspension with brown gummy sticky substance at the bottom. The mixture was sonicated to give a mostly clear solution with a brown solid at the bottom. The solution was decanted and discarded. The solid that remained was rinsed with hexane and then the solid was dried to give **32** (2.7 g, 88%)

1
2
3 as a slightly brown foam. MS(ESI) m/z : 413.1 (M+H)⁺. ¹H NMR (500 MHz, CD₃OD) δ 8.49 (d,
4 $J=5.2$ Hz, 1H), 7.47 (s, 1H), 7.37 (br d, $J=4.4$ Hz, 1H), 7.04 (br d, $J=1.7$ Hz, 1H), 7.03 (d, $J=8.0$
5 Hz, 1H), 6.81 (dd, $J=8.3, 1.9$ Hz, 1H), 5.87 - 5.76 (m, 1H), 5.09 (br d, $J=17.1$ Hz, 1H), 5.05 (br
6 d, $J=10.5$ Hz, 1H), 4.77 - 4.70 (m, 1H), 3.73 (s, 3H), 2.67 - 2.58 (m, 1H), 2.53 - 2.44 (m, 1H),
7 1.42 (s, 9H).

14 Methyl

15
16
17 ***N*-(4-{2-[(1*S*)-1-[(*tert*-butoxy)carbonyl]amino]but-3-en-1-yl}pyridin-4-yl)-3-[(2*R*)-2-methyl**
18 **but-3-enamido]phenyl)carbamate (35)**. To a cooled (-10 °C) solution of **33** (1.20 g, 12.0
19 mmol), **32** (3.30 g, 8.0 mmol), and pyridine (1.9 mL, 24.0 mmol) in EtOAc (40 mL) was added
20 dropwise a solution of T₃P (50 wt% in EtOAc, 9.50 mL, 16.0 mmol). The reaction was stirred at
21 -10 °C and then the reaction was allowed to gradually warm to rt and stir overnight at rt. The
22 reaction mixture was washed with saturated NaHCO₃ (2x). The combined aqueous layers were
23 extracted with EtOAc. The combined EtOAc layers were washed with brine, dried over MgSO₄,
24 filtered, concentrated. Purification by normal phase chromatography (0-50% EtOAc/Hex) gave
25 **35** (4.06 g, 97%) as a white solid. MS (ESI) m/z : 495.1 (M+H)⁺. ¹H NMR (500 MHz, CDCl₃) δ
26 8.61 (d, $J=5.0$ Hz, 1H), 8.15 (d, $J=1.4$ Hz, 1H), 7.56 (br d, $J=7.2$ Hz, 1H), 7.40 (br s, 1H), 7.18
27 (s, 1H), 7.16 (d, $J=8.6$ Hz, 1H), 7.13 (dd, $J=5.0, 1.4$ Hz, 1H), 6.95 (s, 1H), 5.83 - 5.74 (m, 1H),
28 5.74 - 5.65 (m, 1H), 5.56 (br d, $J=7.2$ Hz, 1H), 5.11 - 5.02 (m, 4H), 4.91 - 4.79 (m, 1H), 3.78 (s,
29 3H), 3.10 - 2.98 (m, 1H), 2.68 - 2.56 (m, 2H), 1.44 (s, 9H), 1.27 (d, $J=7.2$ Hz, 3H).

46 Methyl

47
48
49 ***N*-(4-{2-[(1*S*)-1-[(*tert*-butoxy)carbonyl]amino]but-3-en-1-yl}pyridin-4-yl)-3-(2-ethylbut-3-e**
50 **namido)phenyl)carbamate, Diastereomeric mixture (36)**. Using a procedure analogous to that
51 which was used to prepare **30**, compound **32** (0.45 g, 1.09 mmol) was coupled with **34** (0.137 g,
52
53
54
55
56
57
58
59
60

1
2
3 1.20 mmol) to give **36** (0.412 g, 74%) as a mixture of diastereomers and as a white solid. MS
4
5 (ESI) m/z : 509.3 (M+H)⁺. ¹H NMR (500 MHz, CDCl₃) δ 8.61 (d, J =5.0 Hz, 1H), 8.60 (d, J =4.7
6
7 Hz, 1H), 8.15 - 8.10 (m, 2H, NH), 7.60 - 7.51 (m, 2H), 7.42 - 7.34 (m, 2H), 7.20 - 7.12 (m, 6H),
8
9 6.97 (br s, 1H, NH), 6.96 (s, 1H, NH), 5.77 - 5.65 (m, 4H), 5.56 (br d, J =6.1 Hz, 2H, NH), 5.14 -
10
11 5.02 (m, 8H), 4.89 - 4.80 (m, 2H), 3.77 (s, 3H), 3.76 (s, 3H), 2.83 - 2.73 (m, 2H), 2.67 - 2.56 (m,
12
13 4H), 1.93 - 1.82 (m, 2H), 1.61 - 1.49 (m, 2H), 1.44 (s, 18H), 0.90 (t, J =7.4 Hz, 3H), 0.89 (t,
14
15 J =7.4 Hz, 3H).
16
17
18

19 Methyl

20
21 ***N*-[(11*E*,14*S*)-14-{{(*tert*-butoxy)carbonyl}amino}-9-oxo-8,16-diazatricyclo[13.3.1.0^{2,7}]nonade**
22
23 **ca-1(19),2(7),3,5,11,15,17-heptaen-5-yl]carbamate (37)**. To a flame-dried 500 mL RBF was
24
25 added **31** (0.108 g, 0.22 mmol), *p*-toluenesulfonic acid monohydrate (0.047 g, 0.25 mmol), and
26
27 DCM (322 mL). The flask was equipped with a reflux condenser and the clear, colorless solution
28
29 was degassed with argon for 30 min. Next, the reaction was warmed to 40 °C for 1 h. Then a
30
31 solution of Grubbs II (0.038 g, 0.045 mmol) in DCM (2 mL) was added dropwise over 5 min.
32
33 The resulting clear, yellow solution was stirred at 40 °C. After 2 h, the reaction was cooled to rt,
34
35 washed with sat. NaHCO₃, brine, dried over Na₂SO₄, filtered, and concentrated to give dark
36
37 brown solid. Purification by normal phase chromatography (0-75% EtOAc/Hex) gave **37** (0.0554
38
39 g, 53%) as a brown solid. MS (ESI) m/z : 453.3 (M+H)⁺. ¹H NMR (500 MHz, CD₃OD) δ 8.52 (d,
40
41 J =4.9 Hz, 1H), 7.59 (d, J =1.6 Hz, 1H), 7.47 (dd, J =8.2, 2.2 Hz, 1H), 7.39 (d, J =8.2 Hz, 1H), 7.26
42
43 - 7.23 (m, 1H), 6.95 (s, 1H), 5.80 - 5.71 (m, 1H), 4.78 - 4.66 (m, 2H), 3.75 (s, 3H), 2.95 - 2.88
44
45 (m, 1H), 2.83 - 2.74 (m, 1H), 2.66 - 2.58 (m, 1H), 2.25 - 2.15 (m, 1H), 1.42 (s, 9H). ¹H-¹H-
46
47 homonuclear decoupling of the vicinal methylene protons revealed the J coupling constant
48
49 between the double bond protons J = 15.4 Hz.
50
51
52
53
54
55
56
57
58
59
60

Methyl

***N*-[(10*R*,11*E*,14*S*)-14-{{(*tert*-butoxy)carbonyl}amino}-10-methyl-9-oxo-8,16-diazatricyclo[13.3.1.0^{2,7}]nonadeca-1(19),2(7),3,5,11,15,17-heptaen-5-yl]carbamate (38)**. To a flask was added **35** (3.18 g, 6.43 mmol), *p*-toluenesulfonic acid monohydrate (1.34 g, 7.07 mmol), and DCM (540 mL). The flask was equipped with a reflux condenser and the clear yellow solution was degassed with argon for 30 min. The reaction was then warmed to reflux for 1 h. Then a solution of Grubbs II (1.09 g, 1.29 mmol) in DCM (2 mL) was added dropwise. After 4 h, the reaction was cooled to rt, washed with sat. Na₂CO₃, brine, dried over MgSO₄, filtered, and concentrated to give a brown solid. Purification by normal phase chromatography (gradient elution; 0-5% MeOH/DCM) gave **38** (2.19 g, 73%) as a yellow solid. MS (ESI) *m/z*: 467.2 (M+H)⁺. ¹H NMR (500 MHz, CD₃OD) δ 8.52 (d, *J*=5.0 Hz, 1H), 7.54 (s, 1H), 7.46 (dd, *J*=8.5, 2.2 Hz, 1H), 7.39 (d, *J*=8.5 Hz, 1H), 7.25 (dd, *J*=5.0, 1.7 Hz, 1H), 6.90 (s, 1H), 5.70 (ddd, *J*=15.3, 10.6, 4.7 Hz, 1H), 4.60 (br dd, *J*=11.3, 3.6 Hz, 1H), 4.39 (br dd, *J*=15.1, 9.6 Hz, 1H), 3.76 (s, 3H), 3.15 - 3.06 (m, 1H), 2.76 - 2.68 (m, 1H), 2.04 - 1.93 (m, 1H), 1.48 - 1.26 (m, 9H, *t*Bu rotamers), 1.05 (d, *J*=6.6 Hz, 3H).

Methyl

***N*-[(10*R*,11*E*,14*S*)-14-{{(*tert*-butoxy)carbonyl}amino}-10-ethyl-9-oxo-8,16-diazatricyclo[13.3.1.0^{2,7}]nonadeca-1(19),2(7),3,5,11,15,17-heptaen-5-yl]carbamate (39)**. A microwave vial containing a mixture of **36** (0.33 g, 0.65 mmol), Grubbs II (0.110 g, 0.13 mmol) in degassed DCE (16.2 mL) was heated in a microwave at 120 °C for a total of 55 min. The reaction was cooled to rt and concentrated. Purification by normal phase chromatography (gradient elution 0-60% EtOAc/Hex), which allowed for partial separation of the diastereomers, gave **39** (first eluting diastereomer, 0.050 g, 16%) as a brown solid. A mixture of diastereomers (first eluting

1
2
3 and second eluting diastereomer, 0.125 g, 40%) was also obtained. MS (ESI) m/z : 481.2 (M+H)⁺.
4
5 ¹H NMR (400 MHz, CDCl₃) δ 8.66 (d, J =4.9 Hz, 1H), 8.12 (s, 1H), 8.07 (br s, 1H), 7.64 (br d,
6
7 J =6.6 Hz, 1H), 7.39 - 7.29 (m, 2H), 7.17 (dd, J =4.9, 1.1 Hz, 1H), 6.96 (s, 1H), 6.50 (br d, J =7.7
8
9 Hz, 1H, NH), 5.91 - 5.78 (m, 1H), 4.91 (br dd, J =15.4, 9.3 Hz, 1H), 4.79 - 4.68 (m, 1H), 3.79 (s,
10
11 3H), 3.11 - 3.00 (m, 2H), 2.05 - 1.94 (m, 1H), 1.92 - 1.79 (m, 1H), 1.53 - 1.44 (m, 10H), 0.91 -
12
13 0.82 (m, 3H).
14
15

16 Methyl

17
18
19 ***N*-[(14*S*)-14-amino-9-oxo-8,16-diazatricyclo[13.3.1.0^{2,7}]nonadeca-1(19),2(7),3,5,15,17-hexae**
20
21 ***n*-5-yl]carbamate, *Bis*-trifluoroacetic acid salt (**40**).** To a solution of **37** (0.055 g, 0.12 mmol)
22
23 in MeOH (4.9 mL) was added 10% Pd/C (0.019 g, 0.018 mmol). The reaction was purged with
24
25 hydrogen (from a balloon) for several minutes and then the reaction was stirred vigorously under
26
27 a hydrogen atmosphere. After 30 h, the reaction was purged with nitrogen and then the reaction
28
29 was filtered through a 0.45 micron nylon filter, eluting with MeOH. The resulting clear, pink
30
31 filtrate was concentrated to give methyl
32
33

34
35 *N*-[(14*S*)-14- {[(*tert*-butoxy)carbonyl]amino}-9-oxo-8,16-diazatricyclo[13.3.1.0^{2,7}]nonadeca-1(19
36
37),2(7),3,5,15,17-hexaen-5-yl]carbamate (0.056 g, 100%) as a pink solid. MS (ESI) m/z : 455.2
38
39 (M+H)⁺.
40
41

42 A clear, pink solution of methyl

43
44 *N*-[(14*S*)-14- {[(*tert*-butoxy)carbonyl]amino}-9-oxo-8,16-diazatricyclo[13.3.1.0^{2,7}]nonadeca-1(19
45
46),2(7),3,5,15,17-hexaen-5-yl]carbamate (0.055 g, 0.12 mmol) in 30% TFA/DCM (5 mL, 0.12
47
48 mmol) was stirred at rt. After 1 h, the reaction was concentrated to give a residue. The residue
49
50 was dissolved in DCM and concentrated. This process was repeated to give **40** (0.071 g, 100%)
51
52
53
54
55
56
57
58
59
60

1
2
3 as a clear, reddish brown residue. The material was used in the next reaction without further
4
5 purification. MS (ESI) m/z : 355.2 (M+H)⁺.
6
7

8 **Methyl *N*-[(10*R*,14*S*)-14-amino-10-methyl-9-oxo-8,16-diazatricyclo[13.3.1.0^{2,7}]-**
9 **nonadeca-1(19),2(7),3,5,15,17-hexaen-5-yl]carbamate, *Bis*-trifluoroacetic acid salt (41,**
10 **2TFA).** A 1 L hydrogenation flask containing a suspension of **38** (4.53 g, 9.71 mmol) in MeOH
11 (259 mL) and THF (65 mL) was degassed (argon bubbled) for 25 min. To the resulting clear,
12 (259 mL) and THF (65 mL) was degassed (argon bubbled) for 25 min. To the resulting clear,
13
14 light brown solution was added palladium on carbon (10 wt%, wet, 0.947 g, 0.48 mmol) under a
15
16 cone of argon. The flask was purged with nitrogen via an evacuation and backfill (3x). Then the
17
18 flask was pressurized to 55 psi of hydrogen and the reaction was stirred vigorously at rt. After 22
19
20 h, the reaction was stopped, Celite® (10g) and MeOH (250 mL) were added, and the reaction
21
22 was stirred for 10 min. Then, the reaction was filtered through Celite®, eluting with MeOH. The
23
24 filtrate was concentrated to give methyl *N*-[(10*R*,14*S*)-14-{{(*tert*-butoxy)carbonyl}amino}-10-
25
26 methyl-9-oxo-8,16-diazatricyclo[13.3.1.0^{2,7}]nonadeca-1(19),2(7),3,5,15,17-hexaen-5-
27
28 yl]carbamate (4.16 g, 90%) as a gray solid. A portion of the solid was purified by reverse phase
29
30 chromatography which gave methyl *N*-[(10*R*,14*S*)-14-{{(*tert*-butoxy)carbonyl}amino}-10-
31
32 methyl-9-oxo-8,16-diazatricyclo[13.3.1.0^{2,7}]nonadeca-1(19),2(7),3,5,15,17-hexaen-5-
33
34 yl]carbamate, trifluoroacetic acid salt as an analytical sample for characterization. MS (ESI)
35
36 m/z : 469.1 (M+H)⁺. ¹H NMR (500 MHz, CD₃OD, 60 °C) δ 8.65 (d, J =6.1 Hz, 1H), 7.95 (s, 1H),
37
38 7.75 (dd, J =5.9, 1.8 Hz, 1H), 7.59 (d, J =8.3 Hz, 1H), 7.52 (d, J =1.9 Hz, 1H), 7.50 (dd, J =8.5, 2.8
39
40 Hz, 1H), 4.85 (dd, J =10.9, 5.9 Hz, 1H), 3.78 (s, 3H), 2.73 - 2.65 (m, 1H), 2.09 - 2.00 (m, 1H),
41
42 1.86 - 1.69 (m, 2H), 1.57 - 1.44 (m, 2H), 1.39 (s, 9H), 0.95 (d, J =7.2 Hz, 3H), 0.58 - 0.44 (m,
43
44 1H). ¹³C NMR (101 MHz, CD₃OD) δ 176.1, 158.0, 157.4, 156.0, 144.4, 144.2, 137.4, 131.7,
45
46
47
48
49
50
51
52
53
54
55
56
57
58
59
60

1
2
3 128.1, 125.7, 125.2, 118.1, 117.5, 81.5, 54.5, 52.9, 40.3, 32.4, 30.5, 28.7, 20.2, 14.2. Note: two
4
5 carbons overlap. $[\alpha]_{22.6}^D = -40.06$ ($c = 1.11$, MeOH).
6
7

8 A clear, gray solution of methyl *N*-[(10*R*,14*S*)-14-{{(*tert*-butoxy)carbonyl}amino}-10-
9 methyl-9-oxo-8,16-diazatricyclo[13.3.1.0^{2,7}]nonadeca-1(19),2(7),3,5,15,17-hexaen-5-
10 methyl-9-oxo-8,16-diazatricyclo[13.3.1.0^{2,7}]nonadeca-1(19),2(7),3,5,15,17-hexaen-5-
11 yl]carbamate (1.0 g, 2.13 mmol) in DCM (50.8 mL) and TFA (25.4 mL) was stirred at rt. After
12 1h, the reaction was concentrated. The residue was dissolved in DCM and concentrated. This
13 sequence was repeated two more times to give **41**, 2TFA (1.27 g, 100%) as a gray foam. This
14 material was used in the next step without further purification. MS (ESI) m/z : 369.0 (M+H)⁺. ¹H
15 NMR (500 MHz, CD₃OD) δ 8.69 (d, $J=4.7$ Hz, 1H), 7.58 (s, 1H), 7.50 (d, $J=8.3$ Hz, 1H), 7.49 -
16 7.47 (m, 1H), 7.47 - 7.42 (m, 2H), 4.50 (dd, $J=10.7, 5.5$ Hz, 1H), 3.76 (s, 3H), 2.71 - 2.61 (m,
17 1H), 2.15 - 2.05 (m, 1H), 1.86 - 1.67 (m, 2H), 1.48 - 1.32 (m, 2H), 0.94 (d, $J=7.2$ Hz, 3H), 0.62 -
18 0.49 (m, 1H).
19
20
21
22
23
24
25
26
27
28
29
30

31 **Methyl *N*-[(10*R*,14*S*)-14-amino-10-methyl-9-oxo-8,16-diazatricyclo[13.3.1.0^{2,7}]-**
32 **nonadeca-1(19),2(7),3,5,15,17-hexaen-5-yl]carbamate, *Bis*-hydrochloric acid salt (**41**,**
33 **2HCl)**. A flask containing a suspension of methyl *N*-[(10*R*,14*S*)-14-{{(*tert*-butoxy)carbonyl]-
34 amino}-10-methyl-9-oxo-8,16-diazatricyclo[13.3.1.0^{2,7}]nonadeca-1(19),2(7),3,5,15,17-hexaen-5-
35 yl]carbamate (0.250 g, 0.534 mmol) in 4.0 M HCl in dioxane (6.0 mL, 24.0 mmol) was sonicated
36 to give a clear, yellow solution. Then the reaction was stirred at rt. Overtime a precipitate
37 formed. After 30 min, the reaction was filtered to collect the solid. The solid was rinsed with
38 diethyl ether and air-dried to give a hygroscopic solid. The solid was dissolved in MeOH,
39 concentrated, and then lyophilized to give **41**, 2HCl (0.213 g, 90%) as a fluffy, yellow solid. MS
40 (ESI) m/z : 369.0 (M+H)⁺. ¹H NMR (500 MHz, CD₃OD) δ 8.79 (d, $J=5.5$ Hz, 1H), 7.87 (s, 1H),
41 7.70 (dd, $J=5.5, 1.4$ Hz, 1H), 7.57 (d, $J=8.5$ Hz, 1H), 7.54 - 7.48 (m, 2H), 4.71 (dd, $J=11.0, 5.5$
42 Hz, 1H), 3.76 (s, 3H), 2.71 - 2.61 (m, 1H), 2.15 - 2.05 (m, 1H), 1.86 - 1.67 (m, 2H), 1.48 - 1.32 (m, 2H), 0.94 (d, $J=7.2$ Hz, 3H), 0.62 -
43 0.49 (m, 1H).
44
45
46
47
48
49
50
51
52
53
54
55
56
57
58
59
60

1
2
3 Hz, 1H), 3.76 (s, 3H), 2.74 - 2.67 (m, 1H), 2.21 - 2.11 (m, 1H), 2.00 - 1.91 (m, 1H), 1.88 - 1.77
4
5 (m, 1H), 1.56 - 1.37 (m, 2H), 0.95 (d, $J=6.9$ Hz, 3H), 0.63 - 0.50 (m, 1H).
6

7
8 **Methyl *N*-[(10*R*,14*S*)-14-amino-10-ethyl-9-oxo-8,16-diazatricyclo[13.3.1.0^{2,7}]-**
9
10 **nonadeca-1(19),2(7),3,5,15,17-hexaen-5-yl]carbamate, *Bis*-trifluoroacetic acid salt (42).**
11

12 Using a procedure analogous to that which was used to prepare **40**, compound **39** (0.050 g, 0.10
13 mmol) was subjected to hydrogenation conditions to give, after rinsing the Celite® with
14 MeOH/DCM, methyl *N*-[(10*R*,14*S*)-14-{{(*tert*-butoxy)carbonyl]-amino}-10-ethyl-9-oxo-8,16-
15 diazatricyclo[13.3.1.0^{2,7}]nonadeca-1(19),2(7),3,5,15,17-hexaen-5-yl]carbamate (0.045 g, 90%) as
16 a brown solid. MS (ESI) m/z : 483.3 (M+H)⁺.
17
18
19
20
21
22

23
24 Using a procedure analogous to that which was used to prepare **40**, methyl *N*-[(10*R*,14*S*)-
25 14-{{(*tert*-butoxy)carbonyl]-amino}-10-ethyl-9-oxo-8,16-diazatricyclo[13.3.1.0^{2,7}]nonadeca-
26 1(19),2(7),3,5,15,17-hexaen-5-yl]carbamate (0.045 g, 0.093 mmol) was deprotected to give, after
27 purification by reverse phase chromatography, **42** (0.030 g, 53%) as a yellow solid. MS (ESI)
28 m/z : 383.1 (M+H)⁺. ¹H NMR (400 MHz, CD₃OD) δ 8.69 (d, $J=4.9$ Hz, 1H), 7.59 (s, 1H), 7.53 -
29 7.39 (m, 4H), 4.51 (dd, $J=11.0, 5.5$ Hz, 1H), 3.76 (s, 3H), 2.44 - 2.34 (m, 1H), 2.19 - 2.06 (m,
30 1H), 1.80 - 1.66 (m, 2H), 1.59 - 1.45 (m, 1H), 1.44 - 1.30 (m, 2H), 1.30 - 1.17 (m, 1H), 0.85 (t,
31 $J=7.4$ Hz, 3H), 0.75 - 0.56 (m, 1H).
32
33
34
35
36
37
38
39
40
41

42 **Ethyl 1-(3-chloro-2-fluorophenyl)-5-methyl-1*H*-pyrazole-4-carboxylate (49).** To a
43 suspension of (3-chloro-2-fluorophenyl)hydrazine hydrochloride (**46b**, 1.5 g, 7.61 mmol) in
44 EtOH (7.60 mL) was added sequentially ethyl 2-((dimethylamino)methylene)-3-oxobutanoate
45 (1.55 g, 8.37 mmol) followed by TEA (2.12 mL, 15.23 mmol). The resulting clear, dark brown
46 solution was stirred at rt. After 16.5 h, the reaction was concentrated to give a brown residue.
47
48 Purification by normal phase chromatography (gradient elution 0-25% EtOAc/Hex) gave **49**
49
50
51
52
53
54
55
56
57
58
59
60

1
2
3 (0.961 g, 45%) as a yellow solid. MS (ESI) m/z : 283.0 (M+H)⁺. ¹H NMR (500 MHz, CD₃OD) δ
4 8.05 (s, 1H), 7.72 (ddd, $J=8.2, 6.7, 1.7$ Hz, 1H), 7.49 (ddd, $J=8.3, 6.6, 1.7$ Hz, 1H), 7.39 (td,
5
6 $J=8.3, 1.4$ Hz, 1H), 4.33 (q, $J=7.2$ Hz, 2H), 2.44 (d, $J=1.4$ Hz, 3H), 1.37 (t, $J=7.2$ Hz, 3H). ¹⁹F
7
8 NMR (471 MHz, CD₃OD) δ -125.34.
9
10

11
12 **1-(3-Chloro-2-fluorophenyl)-5-methyl-1H-pyrazole-4-carboxylic acid (50)**. A yellow
13
14 suspension of **49** (0.961 g, 3.40 mmol) in MeOH (22.7 mL) and 1.0 M NaOH (13.60 mL, 13.60
15
16 mmol) was warmed to 50 °C. At elevated temperature a clear, yellow-orange solution formed.
17
18 After 2 h, the reaction was cooled to rt and then it was concentrated to give a solid. The solid
19
20 was dissolved in water and then extracted with EtOAc (2x). The aqueous layer was acidified
21
22 with 1.0 N HCl to pH 2-3 which gave a white suspension. The aqueous layer was extracted with
23
24 EtOAc (2x). The second set of organic layers were combined, washed with brine, dried over
25
26 Na₂SO₄, filtered and concentrated to give **50** (0.831 g, 96%) as an off-white solid. MS (ESI)
27
28 m/z : 254.9 (M+H)⁺ and 256.9 (M+2+H)⁺. ¹H NMR (500 MHz, CD₃OD) δ 8.05 (s, 1H), 7.72
29
30 (ddd, $J=8.3, 6.8, 1.7$ Hz, 1H), 7.49 (ddd, $J=8.0, 6.5, 1.7$ Hz, 1H), 7.39 (dt, $J=8.0, 1.6$ Hz, 1H),
31
32 2.44 (d, $J=1.1$ Hz, 3H). ¹⁹F NMR (471 MHz, CD₃OD) δ -125.33. ¹³C NMR (126 MHz, CD₃OD)
33
34 δ 166.5, 154.6 (d, $J=253.2$ Hz), 147.3, 144.1, 133.5, 129.3, 129.0 (d, $J=10.4$ Hz), 126.8 (d, $J=4.6$
35
36 Hz), 123.4 (d, $J=16.2$ Hz), 114.5, 11.3 (d, $J=2.3$ Hz).
37
38
39
40
41
42

43 **1-(3-Chloro-2-fluorophenyl)-5-methyl-1H-imidazole-4-carboxylic acid, HCl salt (52)**.
44

45 Using a modified procedure described by Gomez-Sanchez et al.⁵⁸ A clear, yellow solution of **51**
46
47 (2.90 g, 9.58 mmol) in triethyl orthoformate (96 mL) was degassed with argon for 20 min. Next,
48
49 10% platinum on carbon (0.935 g, 0.48 mmol) was added. The flask was equipped with a reflux
50
51 condenser and the reaction was purged with hydrogen (balloon) for several minutes. The
52
53 reaction was stirred under a hydrogen atmosphere and the reaction was warmed to 75 °C. After 4
54
55
56
57
58
59
60

1
2
3 h, the reaction was cooled to rt. The reaction was placed under vacuum for several minutes and
4
5 then backfilled with argon. The process was repeated a total of 5 times. Next, Celite® was
6
7 added and the reaction was filtered, washing with EtOH. The filtrate was concentrated to give a
8
9 clear, yellow-brown oil weighing 3.17 g. Purification by normal phase chromatography (0-70%
10
11 EtOAc/Hex) provided ethyl 1-(3-chloro-2-fluorophenyl)-5-methyl-1H-imidazole-4-carboxylate
12
13 (1.64 g, 61%) as a white solid. MS (ESI) m/z : 283.0 (M+H)⁺. ¹H NMR (500 MHz, CD₃OD) δ
14
15 7.82 (d, J =0.8 Hz, 1H), 7.73 (ddd, J =8.3, 6.7, 1.8 Hz, 1H), 7.48 (ddd, J =8.0, 6.5, 1.7 Hz, 1H),
16
17 7.43 - 7.38 (m, 1H), 4.36 (q, J =7.2 Hz, 2H), 2.39 (d, J =1.1 Hz, 3H), 1.39 (t, J =7.2 Hz, 3H). ¹⁹F
18
19 NMR (471 MHz, CD₃OD) δ -125.6. ¹³C NMR (126 MHz, CD₃OD) δ 164.7, 154.7 (d, J =252.0
20
21 Hz), 139.1, 138.2, 133.7, 130.4, 129.2, 127.0 (d, J =4.6 Hz), 125.7 (d, J =12.7 Hz), 123.7 (d,
22
23 J =16.2 Hz), 61.7, 14.9, 10.3.

24
25
26 To a clear, colorless solution of ethyl 1-(3-chloro-2-fluorophenyl)-5-methyl-1H-
27
28 imidazole-4-carboxylate (1.64 g, 5.80 mmol) in MeOH (29 mL) was added 1.0 M NaOH (17.4
29
30 mL, 17.4 mmol). The reaction was stirred at rt. After 20 h, the reaction was concentrated under
31
32 high vacuum with minimal heating to give a white solid. The solid was suspended in water and
33
34 1.0 N HCl was added until the mixture was at a pH = 1-2. The solid was collected by filtration
35
36 and rinsed with water, air-dried, and dried under high vacuum to give **52** (1.44 g, 81%) as a
37
38 white solid. MS (ESI) m/z : 255.0 (M+H)⁺ and 257.0 (M+2+H)⁺. ¹H NMR (500 MHz, DMSO- d_6)
39
40 δ 12.35 (br s, 1H), 7.91 - 7.89 (m, 1H), 7.82 (ddd, J =8.2, 6.9, 1.7 Hz, 1H), 7.62 (ddd, J =8.1, 6.9,
41
42 1.5 Hz, 1H), 7.45 (td, J =8.1, 1.4 Hz, 1H), 2.31 (s, 3H). ¹⁹F NMR (471 MHz, DMSO- d_6) δ -124.6.
43
44 ¹³C NMR (126 MHz, DMSO- d_6) δ 164.4, 152.3 (d, J =250.8 Hz), 137.5, 135.8, 131.8, 129.5,
45
46 128.3, 125.9 (d, J =5.8 Hz), 124.3 (d, J =12.7 Hz), 120.9 (d, J =16.2 Hz), 9.8.
47
48
49
50
51
52
53
54
55
56
57
58
59
60

Methyl 1-(3-chloro-2-fluorophenyl)-5-methyl-1*H*-1,2,3-triazole-4-carboxylate (53).

To a cooled (0 °C) purple solution of 3-chloro-2-fluoroaniline (2 g, 13.7 mmol) in TFA (30 mL) and water (6 mL) was added NaNO₂ (0.948 g, 13.7 mmol) in portions over 30 min. Next, NaN₃ (1.79 g, 27.5 mmol) in water was gradually added. Following the addition, the reaction was stirred at 0 °C for 10 min. and then the reaction was allowed to warm to rt. After 2 h, the reaction was quenched with water (100 mL) which gave a suspension. The solid was collected by filtration using a Buchner funnel to give 1-azido-3-chloro-2-fluorobenzene. NOTE: The solid was used immediately in the next step without drying. Arylazides are known to be explosive. Do not use a spatula.

The wet 1-azido-3-chloro-2-fluorobenzene was dissolved in DMSO (10 mL) and water (1 mL). Then, methyl acetoacetate (1.75 g, 15.1 mmol) and piperidine (0.27 mL, 2.8 mmol) were added. The resulting mixture was stirred overnight at rt. Water was added to the reaction which gave a suspension. The solid was collected by filtration and dried to give **53** (3.0 g, 81%) as a white solid. MS (ESI) *m/z*: 269.8 (M+H)⁺. ¹H NMR (300 MHz, DMSO-*d*₆) δ 7.96-7.93 (m, 1H), 7.79-7.73 (m, 1H), 7.57-7.51 (m, 1H), 3.90 (s, 3H), 2.46 (s, 3H).

1-(3-Chloro-2-fluorophenyl)-5-methyl-1*H*-1,2,3-triazole-4-carboxylic acid (54). To a mixture of **53** (2.0 g, 7.4 mmol) in water (20 mL) and MeOH (20 mL) was added NaOH (0.297 g, 7.4 mmol). The reaction was heated overnight at 80 °C. The next day, the reaction was concentrated and then acidified with HCl which gave a suspension. The solid was collected by filtration and dried to give **54** (1.0 g, 53%) as a white solid. MS (ESI) *m/z*: 255.9 (M+H)⁺. ¹H NMR (500 MHz, DMSO-*d*₆) δ 13.31 (br s, 1H), 7.94 (ddd, *J*=8.4, 7.0, 1.7 Hz, 1H), 7.75 (ddd, *J*=8.1, 6.7, 1.7 Hz, 1H), 7.53 (td, *J*=8.2, 1.5 Hz, 1H), 2.44 (d, *J*=0.6 Hz, 3H).

1
2
3 **X-ray crystal structure data collection and structure refinement (see Supporting**
4 **Information Tabulated Data).** X-ray data collection followed that for laboratory sources for
5
6 Corte et al.³³, except that the data were processed using GlobalPhasing, Ltd.'s autoproc
7
8 procedure, which used XDS⁶²⁻⁶³ for integration and, at the time, SCALA⁶⁴ for scaling.
9
10 Refinement followed that of Corte et al.³³ The PDB deposition numbers for compounds **17** and
11
12 **19** complexed to FXIa are 5QTT and 5QTU, respectively.
13
14
15
16
17
18

19 **Enzyme Affinity Assays.** Factors IXa, Xa, XIa, and activated protein C (aPC) were
20
21 purchased from Haematologic Technologies. Factor XIIa, plasmin and recombinant single chain
22
23 tissue-type plasminogen activator (tPA) were purchased from American Diagnostica. Plasma
24
25 kallikrein and α -thrombin were purchased from Enzyme Research Laboratories. Urokinase was
26
27 purchased from Abbott Laboratories. Trypsin was purchased from Sigma Aldrich. Recombinant
28
29 factor VIIa was purchased from Novo Nordisk. Recombinant soluble tissue factor residues 1-219
30
31 was produced at Bristol-Myers Squibb.
32
33
34
35

36 Factor XIa, factor XIIa, tPA, plasmin and urokinase assays were conducted in 50 mM
37
38 HEPES pH 7.4, 145 mM sodium chloride, 5 mM potassium chloride, and 0.1% PEG 8000. Factor
39
40 Xa, thrombin, trypsin, plasma kallikrein, and aPC assays were conducted in 100 mM sodium
41
42 phosphate pH 7.4, 200 mM sodium chloride, and 0.5% PEG 8000. Factor VIIa assays were
43
44 conducted in 50 mM HEPES pH 7.4, 150 mM sodium chloride, 5 mM calcium chloride, and 0.1%
45
46 PEG 8000 containing 40 nM soluble tissue factor. Factor IXa assays were conducted in 50 mM
47
48 TRIS pH 7.4, 100 mM sodium chloride, 5 mM calcium chloride, 0.5% PEG 8000 and 2% DMSO.
49
50 The peptide substrates were: pyro-Glu-Pro-Arg-pNA(*para*-nitroaniline), (Diapharma) for factor
51
52 XIa, thrombin, and aPC; N-benzoyl-Ile-Glu-(OH, OMe)-Gly-Arg-pNA (Diapharma) for factor Xa
53
54
55
56
57
58
59
60

1
2
3 and trypsin; Methylsulfonyl-D-cyclohexylglycyl-Gly-Arg-AMC(7-amino-4-methylcoumarin)
4
5 (Pentapharm) for factor IXa; H-(D)-Ile-Pro-Arg-pNA (Diapharma) for factor VIIa; H-(D)-CHT-
6
7 Gly-Arg-pNA (American Diagnostica) for factor XIIa; H-(D)-Pro-Phe-Arg-pNA (Diapharma) for
8
9 plasma kallikrein; H-(D)-Val-Leu-Lys-pNA (Diapharma) for plasmin; Methylsulfonyl-D-
10
11 cyclohexylalanyl-Gly-Arg-pNA (American Diagnostica) for tPA; and pyro-Glu-Gly-Arg-pNA
12
13 (Diapharma) for urokinase.
14
15
16
17

18 All assays were conducted at 37 °C, except where noted, in 96-well microtiter plate
19
20 spectrophotometers or spectrofluorimeters (Molecular Devices) with simultaneous measurement
21
22 of enzyme activities in control and inhibitor containing solutions. Compounds were dissolved and
23
24 diluted in DMSO and analyzed at a final concentration of 1% DMSO except where noted. Assays
25
26 were initiated by adding enzyme to buffered solutions containing substrate in the presence or
27
28 absence of inhibitor. Hydrolysis of the substrate resulted in the release of pNA (*para*-nitroaniline),
29
30 which was monitored spectrophotometrically by measuring the increase in absorbance at 405 nm,
31
32 or the release of AMC (7-amino-4-methylcoumarin), which was monitored
33
34 spectrofluorometrically by measuring the increase in emission at 460 nm with excitation at 380
35
36 nm. The rate of absorbance or fluorescence change is proportional to enzyme activity. A decrease
37
38 in the rate of absorbance or fluorescence change in the presence of inhibitor is indicative of enzyme
39
40 inhibition. Assays were conducted under conditions of excess substrate (up to 4 times K_m) and
41
42 inhibitor over enzyme. The Michaelis constant, K_m , for substrate hydrolysis by each protease was
43
44 determined by fitting data from independent measurements at several substrate concentrations to
45
46 the Michaelis-Menten equation: $v = (V_{max} * [S]) / (K_m + [S])$ where v is the observed velocity of the
47
48 reaction; V_{max} is the maximal velocity; $[S]$ is the concentration of substrate; K_m is the Michaelis
49
50 constant for the substrate. Values of IC_{50} were determined by allowing the protease to react with
51
52
53
54
55
56
57
58
59
60

1
2
3 the substrate in the presence of the inhibitor. Reactions were allowed to go for periods of 10-120
4 minutes (depending on the protease) and the velocities (rate of absorbance or fluorescence change
5 versus time) were measured. The following relationships were used to calculate IC_{50} values: v_s/v_o
6
7
8
9
10 = $A + ((B-A)/(1 + (IC_{50}/I)^n))$ and where v_o is the velocity of the control in the absence of inhibitor;
11
12 v_s is the velocity in the presence of inhibitor; I is the concentration of inhibitor; A is the minimum
13 activity remaining (usually locked at zero); B is the maximum activity remaining (usually locked
14 at 1.0); n is the Hill coefficient, a measure of the number and cooperativity of potential inhibitor
15 binding sites; IC_{50} is the concentration of inhibitor that produces 50% inhibition. When negligible
16 enzyme inhibition was observed at the highest inhibitor concentration tested the value assigned as
17 a lower limit for IC_{50} is the value that would be obtained with either 25% or 50% inhibition at the
18 highest inhibitor concentration. In all other cases IC_{50} values represent the average of duplicate
19 determinations obtained over 8 to 11 concentrations. The intraassay and interassay variabilities are
20 5% and 20%, respectively. Competitive inhibition was assumed for all proteases. IC_{50} values were
21 converted to K_i values by the relationship: $K_i = IC_{50}/(1 + [S]/K_m)$.
22
23
24
25
26
27
28
29
30
31
32
33
34
35

36 **Coagulation Assays.** Coagulation assays were performed in a temperature-controlled
37 automated coagulation device (Sysmex CA-6000 or CA-1500, Dade-Behring) according to the
38 reagent manufacturer's instructions. Blood was obtained from healthy volunteers by venipuncture
39 and anticoagulated with one-tenth volume 0.11 M buffered sodium citrate (Vacutainer, Becton
40 Dickinson). Plasma was obtained after centrifugation at 2,000 g for 10 minutes and kept on ice
41 prior to use. An initial stock solution of the inhibitor at 10 mM was prepared in DMSO. Subsequent
42 dilutions were done in plasma. Clotting time was determined on control plasma, and plasma
43 containing up to seven different concentrations of inhibitor. Determinations were performed in
44 duplicate and expressed as a mean ratio of treated vs. baseline control. The concentrations required
45
46
47
48
49
50
51
52
53
54
55
56
57
58
59
60

1
2
3 to produce a 50% increase in the clotting time relative to the clotting time in the absence of the
4 inhibitor ($EC_{1.5x}$) were calculated by linear interpolation (Microsoft Excel, Redmond, WA, USA)
5 and are expressed as total plasma concentrations, not final assay concentrations after addition of
6 clotting assay reagents. The aPTT reagent (Actin® FSL) was from commercial sources.
7
8
9
10
11
12
13
14
15
16
17
18
19

20 ASSOCIATED CONTENT

21 Supporting Information

22
23
24 The supporting information is available free of charge on the ACS Publications website:

25
26 <http://pubs.acs.org>. Pharmacokinetic profiles in rat for macrocycles **18-20** (multiple runs);

27
28 Scheme describing the synthesis of the imidazole-based macrocycle **23**; analytical data and

29
30 experimental procedures for compounds **23, 28, 33, 34, 43-45, 47a-c, 48a-e, 51, 56, 57, 59**, and

31
32 **60, 62-65**; experimental procedures for rabbit FXIa affinity assay, rabbit plasma coagulation

33
34 assay, and rabbit ECAT model; overlay of X-ray crystal structures of compounds **17** and **1**; X-

35
36 ray crystal structure of compound **19**; crystallographic data and refinement statistics for X-ray

37
38 crystal structures of the FXIa complexes with compounds **17** and **19**; Molecular formula strings

39
40 (CSV).
41
42
43
44
45
46
47
48

49 AUTHOR INFORMATION

50
51 Corresponding Author

52
53 *E-mail: james.corte@bms.com Phone: 609-466-5030. Fax: 609-818-3331.
54
55
56
57
58
59
60

1
2
3 *E-mail: donald.pinto@bms.com Phone: 609-466-5068. Fax: 609-818-3331.
4
5
6
7
8

9 Notes

10
11
12 The authors declare no competing financial interest. All animal experiments performed in the
13 manuscript were conducted in compliance with institutional guidelines.
14
15
16
17
18

19 **ACKNOWLEDGMENTS**

20
21 The authors thank the Department of Discovery Synthesis for the synthesis of intermediates at
22 BMS Biocon Research Center; the Department of Discovery Synthesis SFC group for chiral
23 separations; the Department of Lead Discovery & Optimization; Mojgan Abousleiman for in
24 vitro work; the Department of Pharmaceutical Candidate Optimization for PK studies and
25 analyses. Gerry Everlof and Theresa Ziembra for solubility determination of selected compounds.
26
27
28
29
30
31
32
33
34
35
36
37
38
39

40 **ABBREVIATIONS USED**

41
42
43
44 FXI, Factor XI; FXIa, Factor XIa; aPTT, activated partial thromboplastin time; $EC_{1.5x}$, effective
45 concentration which produces a 50% increase in the clotting time relative to the clotting time in
46 the absence of the inhibitor; DVT, deep vein thrombosis; ADME, absorption, distribution,
47 metabolism, and excretion; HLM, human liver microsome; RLM, rat liver microsome; DLM,
48 dog liver microsome; CLM, cyno or cynomolgus liver microsome; TPA, tissue plasminogen
49 activator; ECAT, electrically induced carotid artery.
50
51
52
53
54
55
56
57
58
59
60

Accession Codes

Crystallographic structures of **17** and **19** complexed to Factor XIa have been deposited in the PDB as codes 5QTT and 5QTU, respectively. Authors will release the atomic coordinates and experimental data upon article publication.

REFERENCES

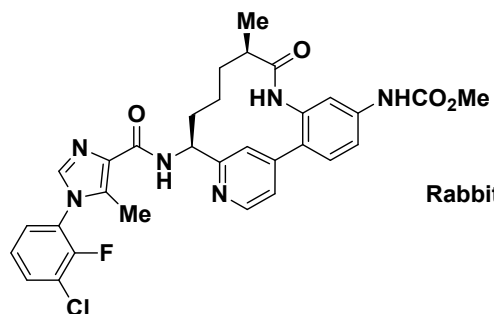
1. GBD Collaborators., Global, regional, and national age-sex-specific mortality for 282 causes of death in 195 countries and territories, 1980-2017: a systematic analysis for the global burden of disease study 2017. *Lancet* **2018**, *392*, 1736-1788.
2. Fox, B. D.; Kahn, S. R.; Langleben, D.; Eisenberg, M. J.; Shimony, A., Efficacy and safety of novel oral anticoagulants for treatment of acute venous thromboembolism: direct and adjusted indirect meta-analysis of randomised controlled trials. *BMJ* **2012**, *345*, e7498.
3. Urooj, F.; Kulkarni, A.; Stapleton, D.; Kaluski, E., New oral anticoagulants in nonvalvular atrial fibrillation. *Clin. Cardiol.* **2016**, *39*, 739-746.
4. Chan, N. C.; Weitz, J. I., Antithrombotic agents. *Circ. Res.* **2019**, *124*, 426-436.
5. Quan, M. L.; Pinto, D. J. P.; Smallheer, J. M.; Ewing, W. R.; Rossi, K. A.; Luetzgen, J. M.; Seiffert, D. A.; Wexler, R. R., Factor XIa inhibitors as new anticoagulants. *J. Med. Chem.* **2018**, *61*, 7425-7447.
6. Bane, C. E.; Neff, A. T.; Gailani, D., Factor XI deficiency or hemophilia C. In *Hemostasis and Thrombosis: Practical Guidelines in Clinical Management*, Saba, H. I., Roberts, H. R., Ed. John Wiley & Sons, Ltd.: Oxford, 2014; pp 71-81.
7. Salomon, O.; Steinberg, D. M.; Zucker, M.; Varon, D.; Zivelin, A.; Seligsohn, U., Patients with severe factor XI deficiency have a reduced incidence of deep-vein thrombosis. *Thromb. Haemost.* **2011**, *105*, 269-273.
8. Salomon, O.; Steinberg, D. M.; Koren-Morag, N.; Tanne, D.; Seligsohn, U., Reduced incidence of ischemic stroke in patients with severe factor XI deficiency. *Blood* **2008**, *111*, 4113-4117.
9. Salomon, O.; Steinberg, D. M.; Dardik, R.; Rosenberg, N.; Zivelin, A.; Tamarin, I.; Ravid, B.; Berliner, S.; Seligsohn, U., Inherited factor XI deficiency confers no protection against acute myocardial infarction. *J. Thromb. Haemost.* **2003**, *1*, 658-661.
10. Doggen, C. J.; Rosendaal, F. R.; Meijers, J. C., Levels of intrinsic coagulation factors and the risk of myocardial infarction among men: opposite and synergistic effects of factors XI and XII. *Blood* **2006**, *108*, 4045-4051.
11. Meijers, J. C.; Tekelenburg, W. L.; Bouma, B. N.; Bertina, R. M.; Rosendaal, F. R., High levels of coagulation factor XI as a risk factor for venous thrombosis. *N. Engl. J. Med.* **2000**, *342*, 696-701.
12. Bane, C. E., Jr.; Gailani, D., Factor XI as a target for antithrombotic therapy. *Drug Discov Today* **2014**, *19*, 1454-1458.
13. Crosby, J. R.; Marzec, U.; Revenko, A. S.; Zhao, C.; Gao, D.; Matafonov, A.; Gailani, D.; MacLeod, A. R.; Tucker, E. I.; Gruber, A.; Hanson, S. R.; Monia, B. P., Antithrombotic effect of antisense factor XI oligonucleotide treatment in primates. *Arterioscler. Thromb. Vasc. Biol.* **2013**, *33*, 1670-1678.

14. Zhang, H.; Lowenberg, E. C.; Crosby, J. R.; MacLeod, A. R.; Zhao, C.; Gao, D.; Black, C.; Revenko, A. S.; Meijers, J. C.; Strokes, E. S.; Levi, M.; Monia, B. P., Inhibition of the intrinsic coagulation pathway factor XI by antisense oligonucleotides: a novel antithrombotic strategy with lowered bleeding risk. *Blood* **2010**, *116*, 4684-4692.
15. Tucker, E. I.; Marzec, U. M.; White, T. C.; Hurst, S.; Rugonyi, S.; McCarty, O. J.; Gailani, D.; Gruber, A.; Hanson, S. R., Prevention of vascular graft occlusion and thrombus-associated thrombin generation by inhibition of factor XI. *Blood* **2009**, *113*, 936-944.
16. Yamashita, A.; Nishihira, K.; Kitazawa, T.; Yoshihashi, K.; Soeda, T.; Esaki, K.; Imamura, T.; Hattori, K.; Asada, Y., Factor XI contributes to thrombus propagation on injured neointima of the rabbit iliac artery. *J. Thromb. Haemost.* **2006**, *4*, 1496-1501.
17. Gruber, A.; Hanson, S. R., Factor XI-dependence of surface- and tissue factor-initiated thrombus propagation in primates. *Blood* **2003**, *102*, 953-955.
18. Wong, P. C.; Crain, E. J.; Watson, C. A.; Schumacher, W. A., A small-molecule factor XIa inhibitor produces antithrombotic efficacy with minimal bleeding time prolongation in rabbits. *J. Thromb. Thrombolysis* **2011**, *32*, 129-137.
19. Schumacher, W. A.; Seiler, S. E.; Steinbacher, T. E.; Stewart, A. B.; Bostwick, J. S.; Hartl, K. S.; Liu, E. C.; Ogletree, M. L., Antithrombotic and hemostatic effects of a small molecule factor XIa inhibitor in rats. *Eur. J. Pharmacol.* **2007**, *570*, 167-174.
20. Lin, J.; Deng, H.; Jin, L.; Pandey, P.; Quinn, J.; Cantin, S.; Rynkiewicz, M. J.; Gorga, J. C.; Bibbins, F.; Celatka, C. A.; Nagafuji, P.; Bannister, T. D.; Meyers, H. V.; Babine, R. E.; Hayward, N. J.; Weaver, D.; Benjamin, H.; Stassen, F.; Abdel-Meguid, S. S.; Strickler, J. E., Design, synthesis, and biological evaluation of peptidomimetic inhibitors of factor XIa as novel anticoagulants. *J. Med. Chem.* **2006**, *49*, 7781-7791.
21. Quan, M. L.; Wong, P. C.; Wang, C.; Woerner, F.; Smallheer, J. M.; Barbera, F. A.; Bozarth, J. M.; Brown, R. L.; Harpel, M. R.; Luetzgen, J. M.; Morin, P. E.; Peterson, T.; Ramamurthy, V.; Rendina, A. R.; Rossi, K. A.; Watson, C. A.; Wei, A.; Zhang, G.; Seiffert, D.; Wexler, R. R., Tetrahydroquinoline derivatives as potent and selective factor XIa inhibitors. *J. Med. Chem.* **2014**, *57*, 955-969.
22. Wong, P. C.; Quan, M. L.; Watson, C. A.; Crain, E. J.; Harpel, M. R.; Rendina, A. R.; Luetzgen, J. M.; Wexler, R. R.; Schumacher, W. A.; Seiffert, D. A., In vitro, antithrombotic and bleeding time studies of BMS-654457, a small-molecule, reversible and direct inhibitor of factor XIa. *J. Thromb. Thrombolysis* **2015**, *40*, 416-423.
23. Hu, Z.; Wong, P. C.; Gilligan, P. J.; Han, W.; Pabbisetty, K. B.; Bozarth, J. M.; Crain, E. J.; Harper, T.; Luetzgen, J. M.; Myers, J. E., Jr.; Ramamurthy, V.; Rossi, K. A.; Sheriff, S.; Watson, C. A.; Wei, A.; Zheng, J. J.; Seiffert, D. A.; Wexler, R. R.; Quan, M. L., Discovery of a potent parenterally administered factor XIa inhibitor with hydroxyquinolin-2(1H)-one as the p2' moiety. *ACS Med. Chem. Lett.* **2015**, *6*, 590-595.
24. Wang, X.; Kurowski, S.; Wu, W.; Castriota, G. A.; Zhou, X.; Chu, L.; Ellsworth, K. P.; Chu, D.; Edmondson, S.; Ali, A.; Andre, P.; Seiffert, D.; Erion, M.; Gutstein, D. E.; Chen, Z., Inhibition of factor XIa reduces the frequency of cerebral microembolic signals derived from carotid arterial thrombosis in rabbits. *J. Pharmacol. Exp. Ther.* **2017**, *360*, 476-483.
25. Pinto, D. J. P.; Orwat, M. J.; Smith, L. M., 2nd; Quan, M. L.; Lam, P. Y. S.; Rossi, K. A.; Apedo, A.; Bozarth, J. M.; Wu, Y.; Zheng, J. J.; Xin, B.; Toussaint, N.; Stetsko, P.; Gudmundsson, O.; Maxwell, B.; Crain, E. J.; Wong, P. C.; Lou, Z.; Harper, T. W.; Chacko, S. A.; Myers, J. E., Jr.; Sheriff, S.; Zhang, H.; Hou, X.; Mathur, A.; Seiffert, D. A.; Wexler, R. R.; Luetzgen, J. M.; Ewing, W. R., Discovery of a parenteral small molecule coagulation factor XIa inhibitor clinical candidate (BMS-962212). *J. Med. Chem.* **2017**, *60*, 9703-9723.
26. Buller, H. R.; Bethune, C.; Bhanot, S.; Gailani, D.; Monia, B. P.; Raskob, G. E.; Segers, A.; Verhamme, P.; Weitz, J. I.; Investigators, F.-A. T., Factor XI antisense oligonucleotide for prevention of venous thrombosis. *N. Engl. J. Med.* **2015**, *372*, 232-240.
27. The rate of bleeding was lower in the FXI-ASO treatment groups compared to the enoxaparin arm, but it was not statistically significant. Due to the modest sample size, this clinical trial was not powered to detect differences in the rate of bleeding.
28. Thomas, D.; Thelen, K.; Kraff, S.; Schwes, S.; Schiffer, S.; Unger, S.; Yassen, A.; Boxnick, S., BAY 1213790, a fully human IgG1 antibody targeting coagulation factor XIa: first evaluation of safety, pharmacodynamics, and pharmacokinetics. *Res Pract Thromb Haemost* **2019**, *3*, 242-253.
29. Xisomab 3G3. <https://clinicaltrials.gov/ct2/show/NCT03612856>. Last accessed September 10, 2019.
30. Koch, A. W.; Schiering, N.; Melkko, S.; Ewert, S.; Salter, J.; Zhang, Y.; McCormack, P.; Yu, J.; Huang, X.; Chiu, Y. H.; Chen, Z.; Schlegler, S.; Horny, G.; DiPetrillo, K.; Muller, L.; Hein, A.; Villard, F.; Scharenberg, M.; Ramage, P.; Hassiepen, U.; Cote, S.; DeGagne, J.; Krantz, C.; Eder, J.; Stoll, B.; Kulmatycki, K.; Feldman, D. L.; Hoffmann, P.; Basson, C. T.; Frost, R. J. A.; Khder, Y., MAA868, a novel FXI antibody with a unique binding mode, shows durable effects on markers of anticoagulation in humans. *Blood* **2019**, *133*, 1507-1516.

- 1
2
3 31. Perera, V.; Luetzgen, J. M.; Wang, Z.; Frost, C. E.; Yones, C.; Russo, C.; Lee, J.; Zhao, Y.; LaCreta, F. P.;
4 Ma, X.; Knabb, R. M.; Seiffert, D.; DeSouza, M.; Mugnier, P.; Cirincione, B.; Ueno, T.; Frost, R. J. A., First-in-human
5 study to assess the safety, pharmacokinetics and pharmacodynamics of BMS-962212, a direct, reversible, small
6 molecule factor XIa inhibitor in non-Japanese and Japanese healthy subjects. *Br. J. Clin. Pharmacol.* **2018**, *84*, 876-
7 887.
- 8 32. Hayward, N. J.; Goldberg, D. I.; Morrel, E. M.; Friden, P. M.; Bokesch, P. M., Abstract 13747: Phase 1a/1b
9 study of EP-7041: a novel, potent, selective, small molecule FXIa inhibitor. *Circulation* **2017**, *136*, A13747-A13747.
- 10 33. Corte, J. R.; Fang, T.; Osuna, H.; Pinto, D. J.; Rossi, K. A.; Myers, J. E., Jr.; Sheriff, S.; Lou, Z.; Zheng, J.
11 J.; Harper, T. W.; Bozarth, J. M.; Wu, Y.; Luetzgen, J. M.; Seiffert, D. A.; Decicco, C. P.; Wexler, R. R.; Quan, M.
12 L., Structure-based design of macrocyclic factor XIa inhibitors: discovery of the macrocyclic amide linker. *J. Med.*
13 *Chem.* **2017**, *60*, 1060-1075.
- 14 34. aPTT (activated partial thromboplastin time) in vitro clotting assay was performed in human plasma. The
15 reported EC_{1.5x} values are the FXIa inhibitor plasma concentrations that produce a 50% increase in the clotting time
16 relative to the clotting time in the absence of the inhibitor.
- 17 35. Ertl, P., Polar surface area. In *Molecular drug properties. measurement and prediction*, Mannhold, R., Ed.
18 Wiley-VCH Verlag GmbH & Co. KGaA: Weinheim, 2008; pp 111-126.
- 19 36. Corte, J. R.; Yang, W.; Fang, T.; Wang, Y.; Osuna, H.; Lai, A.; Ewing, W. R.; Rossi, K. A.; Myers, J. E., Jr.;
20 Sheriff, S.; Lou, Z.; Zheng, J. J.; Harper, T. W.; Bozarth, J. M.; Wu, Y.; Luetzgen, J. M.; Seiffert, D. A.; Quan, M. L.;
21 Wexler, R. R.; Lam, P. Y. S., Macrocyclic inhibitors of factor XIa: discovery of alkyl-substituted macrocyclic amide
22 linkers with improved potency. *Bioorg. Med. Chem. Lett.* **2017**, *27*, 3833-3839.
- 23 37. Clark, C. G.; Rossi, K. A.; Corte, J. R.; Fang, T.; Smallheer, J. M.; De Lucca, I.; Nirschl, D. S.; Orwat, M.
24 J.; Pinto, D. J. P.; Hu, Z.; Wang, Y.; Yang, W.; Jeon, Y.; Ewing, W. R.; Myers, J. E., Jr.; Sheriff, S.; Lou, Z.; Bozarth,
25 J. M.; Wu, Y.; Rendina, A.; Harper, T.; Zheng, J.; Xin, B.; Xiang, Q.; Luetzgen, J. M.; Seiffert, D. A.; Wexler, R. R.;
26 Lam, P. Y. S., Structure based design of macrocyclic factor XIa inhibitors: discovery of cyclic p1 linker moieties with
27 improved oral bioavailability. *Bioorg. Med. Chem. Lett.* **2019**, 126604.
- 28 38. Human liver microsome (HLM) stability and Caco-2 permeability were not determined for macrocycle 3.
29 However, related analogs possessing the cyclic carbamate linker showed poor metabolic stability with HLM T_{1/2} < 18
30 min. Poor permeability with a high efflux ratio in the Caco-2 assay was a common feature for the imidazole-based
31 macrocycles.
- 32 39. Pinto, D. J. P.; Corte, J. R.; Gilligan, P. J.; Fang, T.; Smith, L. M.; Wang, Y.; Yang, W.; Ewing, W. R. Novel
33 macrocycles as factor XIa inhibitors. WO 2013/022818 A1, February 14, 2013.
- 34 40. Wei, Q.; Zheng, Z.; Zhang, S.; Zheng, X.; Meng, F.; Yuan, J.; Xu, Y.; Huang, C., Fragment-based lead
35 generation of 5-phenyl-1H-pyrazole-3-carboxamide derivatives as leads for potent factor XIa inhibitors. *Molecules*
36 **2018**, *23*, 1-23. A phenylpyrazole carboxamide p1 group, which was based on a Bristol-Myers Squibb patent
37 (reference 39), was recently published.
- 38 41. Corte, J. R.; Fang, T.; Pinto, D. J.; Orwat, M. J.; Rendina, A. R.; Luetzgen, J. M.; Rossi, K. A.; Wei, A.;
39 Ramamurthy, V.; Myers, J. E., Jr.; Sheriff, S.; Narayanan, R.; Harper, T. W.; Zheng, J. J.; Li, Y. X.; Seiffert, D. A.;
40 Wexler, R. R.; Quan, M. L., Orally bioavailable pyridine and pyrimidine-based factor XIa inhibitors: discovery of the
41 methyl N-phenyl carbamate p2 prime group. *Bioorg. Med. Chem.* **2016**, *24*, 2257-2272.
- 42 42. Young, M. B.; Barrow, J. C.; Glass, K. L.; Lundell, G. F.; Newton, C. L.; Pellicore, J. M.; Rittle, K. E.;
43 Selnick, H. G.; Stauffer, K. J.; Vacca, J. P.; Williams, P. D.; Bohn, D.; Clayton, F. C.; Cook, J. J.; Krueger, J. A.; Kuo,
44 L. C.; Lewis, S. D.; Lucas, B. J.; McMasters, D. R.; Miller-Stein, C.; Pietrak, B. L.; Wallace, A. A.; White, R. B.;
45 Wong, B.; Yan, Y.; Nantermet, P. G., Discovery and evaluation of potent p1 aryl heterocycle-based thrombin
46 inhibitors. *J. Med. Chem.* **2004**, *47*, 2995-3008.
- 47 43. Ethylene diol is an artifact of the flash-cooling process and is believed to mimic water molecules that mediate
48 H-bonds.
- 49 44. 4- and 6-membered ring linkers were explored but exhibited weaker binding affinities than the pyrazole,
50 unpublished results.
- 51 45. A 3- to 4-fold loss in FXIa binding affinity is typical when comparing Ki values at 37 °C and 25 °C.
- 52 46. Pinto, D. J.; Smallheer, J. M.; Corte, J. R.; Austin, E. J.; Wang, C.; Fang, T.; Smith, L. M., 2nd; Rossi, K. A.;
53 Rendina, A. R.; Bozarth, J. M.; Zhang, G.; Wei, A.; Ramamurthy, V.; Sheriff, S.; Myers, J. E., Jr.; Morin, P. E.;
54 Luetzgen, J. M.; Seiffert, D. A.; Quan, M. L.; Wexler, R. R., Structure-based design of inhibitors of coagulation factor
55 XIa with novel p1 moieties. *Bioorg. Med. Chem. Lett.* **2015**, *25*, 1635-1642.
- 56 47. The combination of the high efflux ratio and poor solubility [$\leq 9.5 \mu\text{g/mL}$, amorphous solids, at pH 6.5 in
57 50 mM phosphate buffer] may account for this variability.

- 1
2
3 48. Wong, P. C.; Pinto, D. J. P.; Zhang, D., Preclinical discovery of apixaban, a direct and orally bioavailable
4 factor Xa inhibitor. *J. Thromb. Thrombolysis* **2011**, *31*, 478-492.
- 5 49. Wong, P. C.; Crain, E. J.; Watson, C. A.; Hua, J.; Schumacher, W. A.; Rehfuss, R., Clopidogrel versus
6 prasugrel in rabbits. effects on thrombosis, haemostasis, platelet function and response variability. *Thromb. Haemost.*
7 **2009**, *101*, 108-115.
- 8 50. Van Lierop, B. J.; Lummis, J. A. M.; Fogg, D. E., Ring-closing metathesis. In *Olefin metathesis: theory and*
9 *practice*, Grela, K., Ed. John Wiley & Sons Inc.: Hoboken, NJ, 2014; pp 85-152.
- 10 51. Negi, S.; Matsukura, M.; Mizuno, M.; Miyake, K.; Minami, N., Synthesis of (2R)-1-(4-chloro-2-pyridyl)-2-
11 (2-pyridyl)ethylamine: a selective oxime reduction and crystallization-induced asymmetric transformation. *Synthesis*
12 **1996**, 991-996.
- 13 52. Sun, X. W.; Liu, M.; Xu, M. H.; Lin, G. Q., Remarkable salt effect on In-mediated allylation of N-tert-
14 butanesulfinyl imines in aqueous media: highly practical asymmetric synthesis of chiral homoallylic amines and
15 isoindolinones. *Org. Lett.* **2008**, *10*, 1259-1262.
- 16 53. Without InCl₃, the addition of allylmagnesium bromide to sulfinimine **25** gave good yields but in modest
17 diastereomeric ratios which varied between 4- to 7: 1.
- 18 54. Kuduk, S. D.; DiPardo, R. M.; Chang, R. K.; Ng, C.; Bock, M. G., Reversal of diastereoselection in the
19 addition of Grignard reagents to chiral 2-pyridyl tert-butyl (Ellman) sulfinimines. *Tetrahedron Lett.* **2004**, *45*, 6641-
20 6643.
- 21 55. Chen, Y.; Dias, H. V. R.; Lovely, C. J., Synthesis of fused bicyclic imidazoles by ring-closing metathesis. .
22 *Tetrahedron Lett.* **2003**, *44*, 1379-1382.
- 23 56. Musser, J. H.; Kubrak, D. M.; Chang, J.; DiZio, S. M.; Hite, M.; Hand, J. M.; Lewis, A. J., Leukotriene D4
24 antagonists and 5-lipoxygenase inhibitors. Synthesis of benzoheterocyclic [(methoxyphenyl)amino]oxoalkanoic acid
25 esters. *J. Med. Chem.* **1987**, *30*, 400-405.
- 26 57. Beck, J. R.; Gajewski, R. P.; Lynch, M. P.; Wright, F. L., Nonaqueous diazotization of 5-amino-1-aryl-1H-
27 pyrazole-4-carboxylate esters. *J. Heterocycl. Chem.* **1987**, *24*, 267-270.
- 28 58. Gomez-Sanchez, A.; Hidalgo, F. J.; Chiara, J. L., Studies on nitroenamines. part III. synthesis and spectral
29 properties of 4-acyl-1-arylimidazoles. *Journal Heterocyclic Chemistry* **1987**, *24*, 1757-1763.
- 30 59. Pokhodylo, N. T.; Shiika, O. Y.; Matiichuk, V. S.; Obushak, N. D., Synthesis of [5-(1H-1,2,3-triazol-4-yl)-
31 1,3,4-oxadiazol-2-yl]pyridines. *Russ. J. Org. Chem.* **2010**, *46*, 417-421.
- 32 60. Bhosale, S.; Kurhade, S.; Prasad, U. V.; Palle, V. P.; Bhuniya, D., Efficient synthesis of isoxazoles and
33 isoxazolines from aldoximes using Magtrieve™ (CrO₂). *Tetrahedron Lett.* **2009**, *50*, 3948-3951.
- 34 61. Roughton, A. L.; Ho, K.-K.; Ohlmeyer, M.; Neagu, I.; Kultgen, S. G.; Ansari, N.; Rong, Y.; Ratcliffe, P. D.;
35 Palin, R. 5-Phenyl-isoxazole-3-carboxamide derivatives as TRPV1 modulators. WO 2009/016241 A1, February 5,
36 2009.
- 37 62. Kabsch, W., XDS. *Acta Crystallogr. D Biol. Crystallogr.* **2010**, *66*, 125-132.
- 38 63. Kabsch, W., Integration, scaling, space-group assignment and post-refinement. *Acta Crystallogr. D Biol.*
39 *Crystallogr.* **2010**, *66*, 133-144.
- 40 64. Evans, P., Scaling and assessment of data quality. *Acta Crystallogr. D Biol. Crystallogr.* **2006**, *62*, 72-82.
- 41
42
43
44
45
46
47
48
49
50
51
52
53
54
55
56
57
58
59
60

Table of Contents Graphic



19
FXIa Ki = 4.1 nM
aPTT EC_{1.5x} = 2.0 μM
Rabbit ECAT ED₅₀ = 1.6 mg/kg + 1 mg/kg/h
%F_{cyno} = 19%